Electrical Power and Energy Systems 152 (2023) 109214

Contents lists available at ScienceDirect

International Journal of Electrical Power and Energy Systems

journal homepage: www.elsevier.com/locate/ijepes

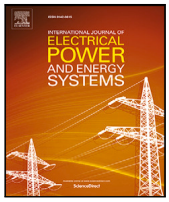

Multi-objective two-stage stochastic unit commitment model for wind-integrated power systems: A compromise programming approach

R. Mena [a,*], M. Godoy [a], C. Catalán [a], P. Viveros [a], E. Zio [b,c]

[a] Department of Industrial Engineering, Universidad Técnica Federico Santa María, Santiago, Chile
[b] MINES Paris-PSL, CRC, Sophia Antípolis, France
[c] Energy Department, Politecnico di Milano, Milano, Italy

ARTICLE INFO

Keywords:
Power systems
Wind energy
Unit commitment
Multi-objective optimization
Stochastic programming
Compromise programming

ABSTRACT

In this paper, we introduce a compromise programming (CP) framework for solving a multi-objective two-stage stochastic unit commitment problem characterized by high penetration of wind power. The proposed framework aims at finding best-compromise Pareto efficient on/off schedules, accounting for wind and power demand uncertainties: such solutions must trade off the three objectives of operating cost, CO_2 emissions, and wind power curtailment in accordance to the decision maker preferences. To achieve this, we introduce a practical procedure to compute the ideal and Nadir points associated to the multi-objective two-stage stochastic unit commitment problem and propose a linearized ℓ_1 norm-based compromise program to design best-compromise on/off schedules that correspondingly minimize and maximize their weighted distances to the ideal point and to the Nadir point, considering the preference weights assigned by the decision maker to each of the three objective functions. The proposed CP framework is applied to a case study related to the New England IEEE-39 bus test system. The results show that, compared to the schedule obtained through the traditional minimization of operating cost, the designed best-compromised schedules considerably improve CO_2 emissions reduction and wind power curtailment performance by conservatively sacrificing operating cost performance.

1. Introduction

Over the last decades, the use of renewable energy sources (RES), such as wind and solar, for producing electrical power has been playing a crucial role in the development of sustainable, low-carbon power systems. In fact, the International Energy Agency (IEA) declared in [1] that solar photovoltaic and wind technologies accounted for approximately the 55% and the 31%, respectively, of the total of 290 GW of new renewable power commissioned in 2021, which represents, in turn, a growth of 3% with respect to the already considerable expansion of 2020. Moreover, the IEA forecasts that in the next five years renewable capacity additions are expected to grow faster than ever. In spite of this, these expansions are not sufficient to meet the Net Zero scenario by 2050. Actually, 2021 experienced a record high of 36.3 Gton energy-related CO_2 emissions [2], due to the extremely rapid economic recovery following the Covid-19 pandemic.

In this scenario, wind power technology is regarded as a relevant option for addressing the urgent challenge of reducing greenhouse gas emissions. The integration of high shares of wind power into existing power systems, nonetheless, introduces challenges with respect to infrastructure planning and operations decisions. Indeed, from an operational point of view, the variable/uncertain nature of wind speed and, consequently, of wind power generation, in association to other sources of uncertainty such as, and in particular, the power demand, delineates a highly dynamic, sequentially time-dependent uncertain operational environment [3]. In such environment, the power system must have a dispatchable generation fleet able to provide sufficient (low-carbon) flexibility, i.e., cycling and ramping capabilities and reserves, to accommodate the high rates of variable wind energy without compromising security and reliability of power supply, while complying with cost-effectiveness and the current ineludible environmental objectives [4].

In line with the above, the traditional frameworks to support operational decision-making for power systems have been extended to take into account the complexities posed by the integration of high shares of variable renewable energy and the additional environmental objectives to fulfill. In this respect, diverse variants of the unit commitment (UC)

* Corresponding author.
E-mail addresses: rodrigo.mena@usm.cl (R. Mena), matias.godoy.14@sansano.usm.cl (M. Godoy), cristobal.catalan@sansano.usm.cl (C. Catalán), pablo.viveros@usm.cl (P. Viveros), enrico.zio@minesparistech.fr, enrico.zio@polimi.it (E. Zio).

https://doi.org/10.1016/j.ijepes.2023.109214
Received 14 October 2022; Received in revised form 23 January 2023; Accepted 27 April 2023
Available online 9 May 2023

Nomenclature

Acronyms and abbreviations

AHP	Analytic hierarchy process.
BPA	Bonneville Power Administration.
CO_2	Carbon dioxide.
CP	Compromise programming.
CCGT	Combined cycle gas turbine.
CST	Coal-fired steam turbine.
OCGT	Open cycle gas turbine.
DM	Decision maker.
IEA	International Energy Agency.
MCDM	Multi-criteria decision-making.
MILP	Mixed-integer linear program.
MO	Multi-objective.
MOO	Multi-objective optimization.
MOOP	multi-objective optimization problem.
NO_x	Nitrogen oxides.
RES	Renewable energy sources.
SO_2	Sulfur dioxide.
UC	Unit commitment.

Sets

$\mathcal{G}$	Set of generation units, indexed by g.
$\mathcal{G}^{\mathrm{l}}$	Set of conventional generation units with a minimum online status duration $t_g^{\mathrm{U}} = 1$, indexed by g.
$\mathcal{G}^{\mathrm{c}}$	Set of conventional generation units, indexed by g.
Ω	Set of operational scenarios, indexed by ξ.
$\mathcal{T}$	Scheduling horizon, indexed by t.
$\mathcal{W}$	Set of wind farms, indexed by g.

Variables

$\Delta P^{\mathrm{D}}_{g,t,\xi} \geq 0$	Downward power output ramp of conventional generation unit g from period $t-1$ to t for scenario ξ, in MW
$\Delta P^{\mathrm{U}}_{g,t,\xi} \geq 0$	Upward power output ramp of conventional generation unit g from period $t-1$ to t for scenario ξ, in MW
$LS_{t,\xi} \geq 0$	Load shedding at period t for scenario ξ, in MW.
$PC^{\mathrm{W}}_{g,t,\xi} \geq 0$	Wind power curtailment at farm g, period t for scenario ξ, in MW.
$P_{g,t,\xi} \geq 0$	Power output of conventional unit g at period t for scenario ξ, in MW.
$p_{g,t,\xi} \geq 0$	Power output above the technical minimum of conventional unit g at period t for scenario ξ, in MW.
$P_{g,t,\xi} \geq 0$	Power used from wind farm g at period t for scenario ξ, in MW.
$r_{g,t,\xi} \geq 0$	Spinning reserve of conventional units g at period t for scenario ξ, in MW.
$u_{g,t} \in \{0,1\}$	Start-up of generation unit g at period t, 1: starts up, 0: otherwise.
$v_{g,t} \in \{0,1\}$	Shut-down of generation unit g at period t, 1: shuts down, 0: otherwise.
$x_{g,t} \in \{0,1\}$	Commitment status of generation unit g at period t, 1: on status, 0: off status.

Parameters

C^{ENS}	Penalty cost for energy not supplied, in US$/MW.
C^{F}_g	Fuel cost of conventional power unit g, in US$/MBtu.
C^{NL}_g	No-load cost of conventional power unit g, in US$/h.
C^{OM}_g	Variable O&M cost of generation unit g, in US$/MWh.
C^{SU}_g	Start-up cost of conventional power unit g, in US$ per installed MW of capacity.
C^{R}_g	Ramping cost of conventional power unit g, in US$/MW.
D_t	Aggregated demand of the system at period t.
$D_{t,\xi}$	Aggregated demand of the system at period t for scenario ξ, in MW.
$\mathcal{G}^{\mathrm{f}}$	Set of fossil fuel-based power units, indexed by g.
H_g	Full load heat rate of conventional unit g, in MBtu/MWh.
μ^{f}_g	Carbon intensity of fossil fuel-based power unit g, in ton/MBtu.
μ_t	Mean of the normally distributed aggregated demand of the system at period t, in MW.
N^{W}_g	Number of wind turbines in farm g.
N^{P}	Number of 2-Pareto efficient solutions to determine.
$P_{g,t,\xi}$	Available power in wind farm g at period t for scenario ξ, in MW.
$\overline{P}_g$	Maximum capacity of conventional unit g, in MW.
$\underline{P}_g$	Technical minimum of conventional unit g, in MW.
P^{R}_g	Rated power of the wind turbines in farm g, in MW.
r^{D}_g	Maximum downward ramp rate of conventional generation unit g, as % of $\overline{P}_g$.
r^{U}_g	Maximum upward ramp rate of conventional generation unit g, as % of $\overline{P}_g$.
$r^{\min}$	Systemic spinning reserve requirements, as % of $D_{t,\xi}$.
r^{SD}_g	Shut-down rate of conventional unit g, in MW.
r^{SU}_g	Start-up rate of conventional unit g, in MW.
σ^2_t	Variance of the normally distributed aggregated demand of the system at period t, in MW^2.
t^{D}_g	Minimum off status duration of generation unit g, in h.
t^{U}_g	Minimum on status duration of generation unit g, in h.
U^{in}_g	Cut-in wind speed of the wind turbines in farm g, in m/s.
U^{out}_g	Cut-in wind speed of the wind turbines in farm g, in m/s.
U^{R}_g	Rated wind speed of the wind turbines in farm g, in m/s.
$\mathbf{w}$	Vector of objective functions weights.
w_k	Weight of the kth objective function.
$ws_{g,t,\xi}$	Wind speed at wind farm's g site at period t for scenario ξ, in m/s.

model have been proposed in recent years for scheduling the dispatchable generation units of a system within a specific short-term time horizon (e.g., 24 or 48 h), while satisfying several technical constraints,

including those sequentially time-dependent (ramping limitations, minimum shut-down and start-up times), to meet a varying power demand with contribution from renewable technologies, and optimizing one or more of different economic, technical and/or environmental objectives [5].

Many direct deterministic approaches have been proposed to address the UC problem with renewables. The most common formulation considers the optimization of a single cost-based (or profit-based) objective function that can include the total operating cost comprising start-up and shut-down, no-load, variable operation and maintenance (O&M) and fuel costs and, in some cases, cost penalties for renewable power curtailment and emissions. In [6], a cost-based UC model is proposed for the security constrained scheduling of hydro-thermal power systems, whereas in [7] cost and profit-based approaches are considered to solve the UC problem with wind power for the tight formulation developed by the authors. Other cost-based UC approaches incorporate cost penalties for renewable power curtailment to the objective function to improve the use of renewable power. In this respect, a network-constrained UC model with dynamic line and transformer ratings in the presence of wind power generation is presented in [8] and a UC comprehensive optimal model considering the costs associated to deep peak regulation of thermal units and wind power curtailment is proposed in [9]. Moreover, the work presented in [10], proposes a UC framework for the flexibility assessment of power systems with high shares of renewable energy. The proposed framework is also cost-based and, beside incorporating penalties for solar and wind energy curtailment, takes into account environmental concerns by including a CO_2 emission cost. It is worth mentioning that, in most of the cases found in the literature, the cost penalties associated to renewable power curtailment and emissions are assumed or arbitrarily defined, with the exception of the work of [9] which presents a methodology to calculate the cost of wind power curtailment.

One way to overcome the above-mentioned arbitrariness consists in enabling the trade-off between two or more objectives through multi-objective optimization (MOO) approaches. In this regard, the commonly proposed MOO frameworks consider the balance of two or three objective quantities in the determination of Pareto optimal generation schedules via deterministic UC models. For instance, a wind-thermal UC model that trade-offs total profit and total emissions is developed in [11]. Similarly, two-objective UC approaches addressing economic and environmental issues consider the balance of total operating cost and NO_x emissions [12], and total operating cost and total emissions [13]. In addition, a multi-objective (MO) UC-based framework for wind and solar integrated power systems is presented in [14], which searches for low carbon Pareto optimal schedules by considering three objective quantities, namely, total operating cost, total CO_2 emissions and sulfur pollutant emissions. Other interesting deterministic UC-based approaches power supply reliability indexes such as the total expected energy not supplied [15] or the loss of load probability [16] as a second objective, on top of an operating cost objective, in the search for optimal schedules compromising those attributes.

Although deterministic single and multi-objective UC model-based approaches hinder the possibility of determining optimal schedules under the variability of RES generation and other sources of uncertainty (e.g. power demand), they provide a solid base-ground for developing UC models considering uncertainty for a robust support to operational decisions. In addition, it is relevant to remark that the above mentioned works acknowledge the fact that, to properly integrate renewable energy into existing power systems, the traditional cost-based decision criteria must be extended to include environmental concerns and the efficient use of RES.

Approaches to the UC problem with renewable generation under uncertainty include scenario-based [17], stochastic [5] and robust techniques [18]. They usually account for uncertainty only in the renewable resource, being wind and solar the most common, or in the demand of power also. Most of the single cost-based objective optimization models under uncertainty in the literature, as for the deterministic models mentioned above, integrate cost penalties associated to emissions or the curtailment of renewable energy to, accordingly, discourage the use of fossil fuels-based generation units (improve emissions performance) or enhance the efficiency in the use of RES. On the one hand, in [19], a stochastic UC model considering the cooperative dispatch of wind power and electric vehicle is presented. Randomness is considered for wind power generation and electric vehicles and the model search to minimize the total expected operating cost including costs for carbon emissions. On the other hand, single objective stochastic UC approaches under wind power uncertainty, that include a cost penalty for wind power curtailment, have been proposed to address diverse challenges imposed by variable renewable energy, such as, the consideration of the risk margin of transmission congestion [20], the impacts on scheduling while studying monthly units start-off schemes [17], the use of bulk energy storage units to provide ramping [21], the quantification of flexibility [22], and the determination of flexible ramp reserves and the associated costs [23]. Similarly, a stochastic UC model under wind power and loads uncertainty is proposed in [24] for coordinated scheduling of generators and tie lines in multi-area power systems.

The concurrent aim of the previous works is to determine scheduling and dispatching decisions regarding conventional generation units, in face of uncertainty, analyzing the contributions of renewable energy to reduce emissions or provide cost-effectiveness, and studying and controlling the impacts on the requirements for enhanced flexibility to reduce or even minimize renewable energy curtailment and the occurrence of congestion in the transmission lines. None of these works, however, considers a conjoint balance between cost-effectiveness, emissions performance and renewable energy curtailment. Indeed, interesting conclusions in this respect are drawn in [4] regarding the misconception that maximizing the use of renewable generation leads always to decrease emissions. Based on a stochastic UC model under wind power uncertainty and considering a cost-based objective function without penalties for emissions or wind energy curtailment, the authors determine that, in some cases, to accommodate the variability of renewables, increased cycling and ramping capabilities can be eventually required from most costly and more pollutant generation units, affecting operating cost and emission performance. The mentioned relevant balance between cost-effectiveness, emissions performance and renewable energy curtailment has not been considered also in MOO approaches to the UC problem with renewable generation under uncertainty. For instance, in [25] the MO unit commitment problem of jointly concentrating solar and wind technologies for providing peak-shaving is addressed. The corresponding optimization model seeks the simultaneous minimization of two objectives, namely, the peak-shaving performance and the operational risk of incurring in wind power curtailment and energy not served. Similarly, MOO UC model under stochastic and fuzzy uncertainties associated to the occurrence of failures and wind power and load forecasts, respectively, have been proposed to determine schedules that balance a cost-based objective including the cost for CO_2, SO_2 and NO_x emissions trading or treatment and the risk of incurring in unreliable supply of power, measured by means of the value-at-risk [26], the conditional value-at-risk [27] and the fuzzy value-at-risk [28]. Moreover, in [29], a three-objective function MOO approach is proposed, seeking to minimize operating cost, coal consumption and SO_2, but neglecting the efficient use of wind power.

In regards to the methods of solution of the UC problem with renewable generation, most single-objective approaches, both deterministic and under uncertainty, formulate the problem in terms of mixed-integer linear programs (MILP) and resort to traditional exact techniques of optimization based on the branch and bound/cut method [18] or to approximative metaheuristics based on evolutionary algorithms such as adaptive genetic algorithms [6] (GA), memetic algorithms (MA) [17] and particle swarm optimization (PSO) [9],

among others. Exact methods of solution guarantee optimality but at the expense of higher computational requirements that can hinder their implementation on large scale power systems [20]. Conversely, metaheuristics techniques can provide good-quality solutions in reasonable computational times but with additional efforts regarding parameters configuration [30] and constraint handling [6]. Considering that even for MILP formulations the UC problem can be considered as NP-hard [31] and, given the increased complexity MOUC with renewable integration approaches, *a posteriori* metaheuristic techniques like memetic binary differential evolution (MBDE) [11], fuzzy simulation-based PSO (FS-PSO) [27], ϵ-MOGA [32], non-dominated sorting GA-III (NSGA-III) [14], MA-GA [13], among others, are commonly proposed to tackle this kind of problem. An application of an exact *posteriori* MOO method of solution through the Tchebycheff approach is proposed in [25]. These approximative or exact *a posteriori* MOO techniques search to approximate or construct the set of Pareto efficient solutions associated to a MOUC problem, conveying substantial information to the decision maker (DM) before he/she establishes his/her preferences [33], but requiring high computational efforts and the potential information overload of the decision maker when deciding on his/her most preferred solution [34].

In this paper, we address the challenge of modeling the operation of a power system with high shares of wind power. For this, and with the need of conjointly balancing key operational attributes identified in the reviewed literature, we propose a multi-objective two-stage stochastic unit commitment model, under wind resource and power demand uncertainties, aiming at the simultaneous minimization of three conflicting objectives: (expected) operating cost, CO_2 emissions and wind power curtailment. In this view, the contributions of this work are:

- The design and implementation of an *a priori* exact MOO framework, based on compromise programming (CP), that aims at finding Pareto optimal on/off schedules that trade-off the three mentioned objectives under the realistic premise that the decision maker (DM), according to his/her predefined preferences, seeks tailored Pareto optimal schedules as close as possible to the ideal point, i.e., to the theoretical point where the three objectives are simultaneously minimized, and as far as possible to the anti-ideal or Nadir point, i.e., to the point where the three objectives are concurrently maximized.
- The introduction of a comprehensible and practical procedure to compute the ideal and Nadir points, and the trade-off ranges of each of the three objective functions associated to the proposed multi-objective two-stage stochastic unit commitment problem, based on an augmented ϵ-constrained method that integrates a normalized euclidean distance-based bisection routine to generate more equispaced Pareto fronts.
- The formulation of a weighted ℓ_1 norm-based linearized compromise program that allows to design best-compromise on/off schedules that minimize/maximize their distances to the ideal/Nadir point in accordance to the DM's preferences, which are represented by weights of relative importance of the three objectives considered.

We apply the proposed CP framework to a case study based on a modification of the New England IEEE-39 bus test system, and discussing its effectiveness and implications by comparison of the best-compromised on/schedules against the schedule obtained via traditional minimization of the expected operating cost.

The remainder of this paper is organized as follows. In Section 2, the tight and compact MILP formulation of the multi-objective two-stage stochastic UC model is presented. In Section 3, important definitions for compromised programming are introduced, the procedures for computing the ideal and Nadir points are presented as and the formulation of the mathematical program for designing best-compromise solutions is given. Section 4, presents the results of the application of the proposed CP framework to the case study. Concluding remarks are given in Section 5.

2. Mathematical formulation

In this section, we describe the proposed tight and compact MILP formulation of the two-stage stochastic UC model, which is based on the work of [7]. For this, we based on the deterministic equivalent or extensive formulation of the problem.

We consider the power system to be composed by a set of generation units $\mathcal{G}$ grouped into two subsets, $\mathcal{G}^{\mathrm{c}}$ and $\mathcal{W}$, denoting conventional/dispatchable generation units and wind farms, respectively. The aim of the stochastic UC model is to construct an optimal on/off schedule of the conventional generation units within a specific short-term time horizon $\mathcal{T}$, determining their power output for each instant $t \in \mathcal{T}$, so as to meet the system uncertain demand profile given the also uncertain availability of wind power throughout $\mathcal{T}$. This is sought while satisfying several technical and operational constraints, such as generators minimum and maximum capacities, ramping limits, minimum shut-down and start-up times, reserves, etc.

The stochastic parameters considered are the system power demand, D_t MW, and the wind speed profiles $ws_{g,t}$ m/s for each wind farm $g \in \mathcal{W}$ present in the system. The diverse scenarios of these parameters are represented by the set Ω. The modeling of the stochastic behavior of these parameters and the formulation of the stochastic UC model are presented in the following.

2.1. Stochastic parameters

2.1.1. System demand

The aggregated demand of the system D_t MW for each period t within the scheduling horizon $\mathcal{T}$, is considered as normally distributed with mean μ_t and variance σ_t^2 [35]. Then, realizations of the aggregated demand profiles $\{D_{t,\xi}\}_{t=1,\ldots,|T|}$ with $\xi \in \Omega$ are sampled from the normal distributions corresponding to each period $t \in \mathcal{T}$.

2.1.2. Wind speed

For each wind farm $g \in \mathcal{W}$, discrete wind speed time series $\{ws_{g,t,\xi}\}_{t=1,\ldots,|T|}$ m/s are synthesized by means of the Matérn stochastic process [36] for each scenario $\xi \in \Omega$. Then, to determine the series of available wind power $\{P^{\mathrm{W}}_{g,t,\xi}\}_{t=1,\ldots,|T|}$ MW at each wind farm, the sampled wind speed time series are given in input to a wind energy conversion model, presented in (1):

$$P^{\mathrm{W}}_{g,t,\xi} = \begin{cases} 0 & 0 < ws_{g,t,\xi} < U^{\mathrm{in}} \\ N^{\mathrm{W}}_g P^{\mathrm{R}} \dfrac{ws_{g,t,\xi} - U^{\mathrm{in}}_g}{U^{\mathrm{R}}_g - U^{\mathrm{in}}_g} & U^{\mathrm{in}}_g \le ws_{g,t,\xi} < U^{\mathrm{R}}_g \\ N^{\mathrm{W}}_g P^{\mathrm{R}}_g & U^{\mathrm{R}}_g \le ws_{g,t,\xi} < U^{\mathrm{out}}_g \\ 0 & \text{otherwise} \end{cases} \quad \forall g \in \mathcal{W}, t \in \mathcal{T}, \xi \in \Omega \tag{1}$$

where N^{W}_g is the number of wind turbines in farm $g \in \mathcal{W}$, P^{R}_g MW is the rated power of the wind turbines, and U^{in}_g m/s, U^{R}_g m/s and U^{out}_g m/s are the corresponding cut-in, rated and cut-out wind speeds.

2.2. Constraints

2.2.1. Commitment

The first stage of the proposed UC model regards commitment decisions on the on/off status of conventional generation units, restricted by the following sets of logical constraints:

$$x_{g,t} - x_{g,t-1} = u_{g,t} - v_{g,t}, \qquad \forall g \in \mathcal{G}^{\mathrm{c}}, t \in \mathcal{T}, t \ge 2 \tag{2}$$

$$\sum_{\tau=t-t^{\mathrm{U}}_g+1}^{t} u_{g,\tau} \le x_{g,t}, \qquad \forall g \in \mathcal{G}^{\mathrm{c}}, t \in \mathcal{T}, t \ge t^{\mathrm{U}}_g \tag{3}$$

$$\sum_{\tau=t-t^{\mathrm{D}}_g+1}^{t} v_{g,\tau} \le 1 - x_{g,t}, \qquad \forall g \in \mathcal{G}^{\mathrm{c}}, t \in \mathcal{T}, t \ge t^{\mathrm{D}}_g \tag{4}$$

where, $x_{g,t}$ are binary decision variables for the committed status of generation unit g at period t, taking the value 1 if the unit is in *on* status and 0 otherwise, $u_{g,t}$ and $v_{g,t}$ are also binary decision variables representing, respectively, the start-up and shut-down of generation unit g at period t, taking correspondingly the value 1 if the unit is started-up or shut-down.

Constraints set (2) relates the on/off status variables $x_{g,t}$ with the start-up and shut-down decisions $u_{g,t}$ and $v_{g,t}$ throughout time. Constraint set (3) forces generation unit g to stay in *on* status for at least t_g^{U} consecutive periods, before it can be shut-down and, analogously, constraint set (4) ensures the minimum *off* status duration of unit g to be greater or equal to t_g^{D}. It is worth mentioning that constraints sets (3) and (4) guarantee that conventional generation unit g cannot be started-up and shut-down simultaneously [37].

2.2.2. Power balance

The second stage of the model considers decisions on the power output of generation units, after the realization of the uncertainty associated to the system power demand and wind speed profiles. In this regard, the first set of constraints (5) ensures the satisfaction of the system power demand for each period $t \in \mathcal{T}$ and each sampled scenario $\xi \in \Omega$,

$$\sum_{g\in\mathcal{G}^{\mathrm{c}}} P_{g,t,\xi} + \sum_{g\in\mathcal{W}} P_{g,t,\xi} + LS_{t,\xi} = D_{t,\xi}, \quad \forall t \in \mathcal{T}, \xi \in \Omega \tag{5}$$

where $P_{g,t,\xi} \geq 0$ are decision variables representing either the power output in MW of conventional generator $g \in \mathcal{G}^{\mathrm{c}}$ or the power used from wind farm $g \in \mathcal{W}$ at period t for the scenario ξ and $LS_{t,\xi} \geq 0$ are decision variables defining the load shedding in MW at period t for the scenario ξ.

It is worth mentioning that for conventional generation units $g \in \mathcal{G}^{\mathrm{c}}$, the decision variables $P_{g,t,\xi}$ are defined as auxiliary based on the unit g committed status $x_{g,t}$ at a given period t and its technical minimum $\underline{P}_g$ in MW and decision variables $p_{g,t,\xi} \geq 0$ representing the power output above the technical minimum of unit g at period t for the scenario ξ. Then, the total power output can be expressed as $P_{g,t,\xi} = \underline{P}_g x_{g,t} + p_{g,t,\xi}$. The decision variables $p_{g,t,\xi} \geq 0$ are useful to formulate tighter and more compact generation limits constraints taking into account the start-up and shut-down capabilities of conventional units, as presented in the following section.

2.2.3. Generation limits

The limit of the power output above the technical minimum $p_{g,t,\xi}$ of conventional units g at period t for scenario ξ is stated by constraints sets (6) and (7):

$$p_{g,t,\xi} \leq (\overline{P}_g - \underline{P}_g)x_{g,t} - (\overline{P}_g - r_g^{\mathrm{SU}})u_{g,t} - (\overline{P}_g - r_g^{\mathrm{SD}})v_{g,t+1} - r_{g,t,\xi},$$
$$\forall g \in \mathcal{G}^{\mathrm{c}} \setminus \mathcal{G}^{1}, t \in \mathcal{T}, t \leq |\mathcal{T}| - 1, \xi \in \Omega \tag{6}$$
$$p_{g,t,\xi} \leq (\overline{P}_g - \underline{P}_g)x_{g,t} - (\overline{P}_g - r_g^{\mathrm{SU}})u_{g,t} - r_{g,t,\xi},$$
$$\forall g \in \mathcal{G}^{\mathrm{c}} \setminus \mathcal{G}^{1}, t \in \mathcal{T}, t = |\mathcal{T}|, \xi \in \Omega \tag{7}$$

where $\overline{P}_g$ and $\underline{P}_g$ MW are correspondingly the maximum capacity and technical minimum of conventional unit g, whereas r_g^{SU} and r_g^{SD} MW are its respective start-up and shut-down rates, $r_{g,t,\xi} \geq 0$ MW are decision variables defining the spinning reserve for conventional units g at period t for scenario ξ.

Constraints sets (6) and (7) establish that the power output above the technical minimum for conventional unit g at period t for the scenario ξ is limited by $r_g^{\mathrm{SU}} - \underline{P}_g$, $r_g^{\mathrm{SD}} - \underline{P}_g$ or $\overline{P}_g - \underline{P}_g$, when the unit is started-up at period t, or shut-down at period $t+1$, or it has remained in *on* status for a number of periods up to t, respectively. This is done while also ensuring a level of spinning reserve equal to $r_{g,t,\xi}$. It must be pointed out that these constraints are invalid for conventional units with a minimum online status duration $t_g^{\mathrm{U}} = 1$ period, i.e., $g \in \mathcal{G}^{1} \subset \mathcal{G}$, because cases with $x_{g,t} = u_{g,t} = 1$ and $v_{g,t+1} = 1$ could lead to infeasibility due to possible negative values in the right side of the inequality (6). This is why constraints sets (6) and (7) are applied only over the set $g \in \mathcal{G}^{\mathrm{c}} \setminus \mathcal{G}^{1}$, which considers conventional generation units with $t_g^{\mathrm{U}} \geq 2$.

For conventional units $g \in \mathcal{G}^{1}$, i.e., with $t_g^{\mathrm{U}} = 1$, the limit of the power output above the technical minimum is modeled by constraints sets (8)–(11).

$$p_{g,t,\xi} \leq (\overline{P}_g - \underline{P}_g)x_{g,t} - (\overline{P}_g - r_g^{\mathrm{SU}})u_{g,t} - \max\{r_g^{\mathrm{SU}} - r_g^{\mathrm{SD}}, 0\}v_{g,t+1} - r_{g,t,\xi},$$
$$\forall g \in \mathcal{G}^{1}, t \in \mathcal{T}, t \leq |\mathcal{T}| - 1, \xi \in \Omega \tag{8}$$
$$p_{g,t,\xi} \leq (\overline{P}_g - \underline{P}_g)x_{g,t} - \max\{r_g^{\mathrm{SD}} - r_g^{\mathrm{SU}}, 0\}u_{g,t} - (\overline{P}_g - r_g^{\mathrm{SD}})v_{g,t+1} - r_{g,t,\xi},$$
$$\forall g \in \mathcal{G}^{1}, t \in \mathcal{T}, t \leq |\mathcal{T}| - 1, \xi \in \Omega \tag{9}$$
$$p_{g,t,\xi} \leq (\overline{P}_g - \underline{P}_g)x_{g,t} - (\overline{P}_g - r_g^{\mathrm{SU}})u_{g,t} - r_{g,t,\xi},$$
$$\forall g \in \mathcal{G}^{1}, t \in \mathcal{T}, t = |\mathcal{T}|, \xi \in \Omega \tag{10}$$
$$p_{g,t,\xi} \leq (\overline{P}_g - \underline{P}_g)x_{g,t} - \max\{r_g^{\mathrm{SD}} - r_g^{\mathrm{SU}}, 0\}u_{g,t} - r_{g,t,\xi},$$
$$\forall g \in \mathcal{G}^{1}, t \in \mathcal{T}, t = |\mathcal{T}|, \xi \in \Omega \tag{11}$$

Constraint set (12) defines the power balance (or generation limits) for a wind farm $g \in \mathcal{W}$ ensuring that the power used from the farm $P_{g,t,\xi}$ and the amount of power curtailed $PC_{g,t,\xi}^{\mathrm{W}}$ must equal the available wind power at period t for scenario ξ, as expressed below:

$$P_{g,t,\xi} + PC_{g,t,\xi}^{\mathrm{W}} = P_{g,t,\xi}^{\mathrm{W}}, \quad \forall g \in \mathcal{W}, t \in \mathcal{T}, \xi \in \Omega \tag{12}$$

where $PC_{g,t,\xi}^{\mathrm{W}} \geq 0$ are decision variables representing the wind power curtailment in MW at farm g, at period t for scenario ξ.

2.2.4. Ramping limits

The sets of constraints (13) and (14) limit, respectively, the upward and downward ramping capacities of conventional power units $g \in \mathcal{G}$:

$$p_{g,t,\xi} - p_{g,t-1,\xi} \leq r_g^{\mathrm{U}}\overline{P}_g - r_{g,t,\xi}, \qquad \forall g \in \mathcal{G}^{\mathrm{c}}, t \in \mathcal{T}, t \geq 2, \xi \in \Omega \tag{13}$$
$$p_{g,t-1,\xi} - p_{g,t,\xi} \leq r_g^{\mathrm{D}}\overline{P}_g, \qquad \forall g \in \mathcal{G}^{\mathrm{c}}, t \in \mathcal{T}, t \geq 2, \xi \in \Omega \tag{14}$$

where r_g^{U} and r_g^{D} are the maximum upward and downward ramp rates of conventional generation unit g, defined as a percentage of its maximum capacity $\overline{P}_g$.

Constraint set (15) ensures the estimation of the excluding non-negative or non-positive power output ramp provided by a conventional generation unit g from period $t-1$ to t for the scenario ξ. This is formulated for evaluating the associated ramping costs:

$$P_{g,t,\xi} - P_{g,t-1,\xi} = \Delta P_{g,t,\xi}^{\mathrm{U}} - \Delta P_{g,t,\xi}^{\mathrm{D}}, \quad \forall g \in \mathcal{G}^{\mathrm{c}}, t \in \mathcal{T}, t \geq 2, \xi \in \Omega \tag{15}$$

where $\Delta P_{g,t,\xi}^{\mathrm{U}} \geq 0$ and $\Delta P_{g,t,\xi}^{\mathrm{D}} \geq 0$ are decision variables representing the magnitudes in MW of the upward and downward power output ramp of conventional generation unit g from period $t-1$ to t for the scenario ξ.

2.2.5. Spinning reserve

The systemic spinning reserve requirement at period t is established as a percentage $r^{\min}$ of the power demand and its satisfaction is guaranteed by constraints set (16):

$$r^{\min} D_{t,\xi} \leq \sum_{g\in\mathcal{G}^{\mathrm{c}}} r_{g,t,\xi}, \quad \forall t \in \mathcal{T}, \xi \in \Omega \tag{16}$$

2.3. Objective functions

The proposed two-stage stochastic UC model considers three objective functions to be concurrently minimized, corresponding to the expected value of total operating cost, total CO_2 emissions and total wind power curtailment given the set of scenarios Ω with probability of occurrence $\mathbf{P}_{\xi}$.

2.3.1. Expected total operating cost

The total operating cost of the system C_{ξ}^{T} in US$ for the scenario $\xi \in \Omega$ within the scheduling horizon $\mathcal{T}$ considers start-up, no-load, variable O&M and fuel costs of conventional power generation units, and also the costs of providing ramping. Moreover, this quantity takes into account the variable O&M associate to wind farms and a penalty for energy not supplied. Then, the expected value of C_{ξ}^{T} is formulated below:

$$\begin{aligned}\min_{\mathbf{x}} \quad f_1(\mathbf{x}) &= \mathbf{E}(C_{\xi}^{\mathrm{T}}) \\ &= \sum_{\xi\in\Omega} \mathbf{P}_{\xi} \left\{ \sum_{t\in\mathcal{T}} \sum_{g\in\mathcal{G}^{\mathrm{c}}} C_g^{\mathrm{SU}} \overline{P}_g u_{g,t} \right. \\ &+ C_g^{\mathrm{NL}} x_{g,t} + (C_g^{\mathrm{OM}} + C_g^{\mathrm{F}} H_g) P_{g,t,\xi} \Delta t + \\ &\sum_{t\in\mathcal{T}} \sum_{g\in\mathcal{G}^{\mathrm{c}}} C_g^{\mathrm{R}} (\Delta P_{g,t,\xi}^{\mathrm{U}} + \Delta P_{g,t,\xi}^{\mathrm{D}}) + \sum_{t\in\mathcal{T}} \sum_{g\in\mathcal{W}} C_g^{\mathrm{OM}} P_{g,t,\xi} \Delta t \\ &\left. + \sum_{t\in\mathcal{T}} C^{\mathrm{ENS}} LS_{t,\xi} \Delta t \right\}\end{aligned} \tag{17}$$

where C_g^{SU} is the start-up cost of conventional power unit $g \in \mathcal{G}$ in US$ per installed MW of capacity, and C_g^{NL} US$/h, C_g^{OM} US$/MWh and C_g^{F} US$/MBtu, are its no-load, variable O&M and fuel costs, respectively. H_g is the full load heat rate of conventional unit g in MBtu/MWh associated to the fuel used by it. In addition, C_g^{R} is the ramping cost in US$/MW of conventional unit g. On the other hand, C_g^{OM} US$/MWh for $g \in \mathcal{W}$ denotes the variable O&M of wind farm g and C^{ENS} is the penalty cost for energy not supplied expressed in US$/MWh.

2.3.2. Expected total CO_2 emissions

The total amount of CO_2 emissions resulting from the operation of the system $E^{\mathrm{TCO_2}}$ (Mton) for the scenario $\xi \in \Omega$ within the scheduling horizon $\mathcal{T}$ is measured based on the set $\mathcal{G}^{\mathrm{f}}$ that includes all fossil fuel-based conventional power units g. The expected value of $E^{\mathrm{TCO_2}}$ is given by Eq. (18).

$$\min_{\mathbf{x}} \quad f_2(\mathbf{x}) = \mathbf{E}(E_{\xi}^{\mathrm{TCO_2}}) = \sum_{\xi\in\Omega} \mathbf{P}_{\xi} \left\{ \sum_{t\in\mathcal{T}} \sum_{g\in\mathcal{G}^{\mathrm{f}}} H_g \mu_g^{\mathrm{f}} P_{g,t,\xi} \Delta t \right\} \tag{18}$$

where, μ_g^{f} is the carbon intensity in ton/MBtu associated to the fossil fuel used by conventional power unit $g \in \mathcal{G}^{\mathrm{f}}$.

2.3.3. Expected total wind power curtailment

The total wind power curtailed PC_{ξ}^{TW} in MW for the scenario $\xi \in \Omega$ within the scheduling horizon $\mathcal{T}$ is defined as the aggregation of the power curtailed at each wind farm, and its expected value is obtained through Eq. (19):

$$\min_{\mathbf{x}} \quad f_3(\mathbf{x}) = \mathbf{E}(PC_{\xi}^{\mathrm{TW}}) = \sum_{\xi\in\Omega} \mathbf{P}_{\xi} \left\{ \sum_{t\in\mathcal{T}} \sum_{g\in\mathcal{W}} PC_{g,t,\xi}^{\mathrm{W}} \right\} \tag{19}$$

3. Compromise programming

As stated in the Introduction, the objective of the present work is to develop a CP framework to determine an optimal solution to the MO two-stage stochastic UC problem which is as close as possible to the theoretical ideal solution, i.e., to the solution that simultaneously minimizes the three proposed objective functions, and/or which is as far as possible to the theoretical anti-ideal solution or Nadir point, i.e., to the solution where the three objective functions are concurrently maximized, or to design optimal solutions that trade-off these objectives based on the DM preferences. Evidently, the solution(s) to be determined or designed must belong to the Pareto-efficient set associated to the given multi-objective optimization problem (MOOP), thus, calling for the integration of Pareto optimal concepts, which are, in turn, the base is to define the ideal and Nadir points.

3.0.1. Pareto efficiency

In general, solving a MOOP of the form given below, with at least two conflicting objective functions $f_k : \mathbb{R}^n \to \mathbb{R}, \forall k \in \{1,\dots,K\}$, implies to find a subset of feasible solutions $\mathbf{x}^* \in \mathcal{D} \subset \mathbb{R}^n$ such that it does not exist another feasible solution $\mathbf{x}$ that dominates $\mathbf{x}^*$ or that is at least as good as any $\mathbf{x}^*$ with respect to all objective functions and strictly better for at least one of them [38], as defined in (20):

$$\begin{aligned}\min_{\mathbf{x}} \quad & (f_1(\mathbf{x}),\dots,f_K(\mathbf{x}))^T \\ \text{s.t.} \quad & \mathbf{x} \in \mathcal{D}\end{aligned} \tag{MOOP}$$

The feasible solutions $\mathbf{x}^*$ that satisfy (20) are called Pareto optimal or Pareto efficient. The set of Pareto efficient solutions associated to the problem (MOOP) is denoted by Λ^{P}:

$$\begin{aligned}&\nexists \mathbf{x} \in \mathcal{D} : f_k(\mathbf{x}) \le f_k(\mathbf{x}^*),\ \forall k \in \{1,\dots,K\} \\ &\text{and } f_k(\mathbf{x}) < f_k(\mathbf{x}^*) \text{ for at least one } k\end{aligned} \tag{20}$$

Another important definition regards weakly Pareto efficiency. A feasible solution $\mathbf{x}^*$ of the problem (MOOP) is called weakly Pareto optimal if it does not exist another feasible solution $\mathbf{x}$ which is strictly better with respect to all objective functions [38], i.e, $\mathbf{x}^*$ satisfies the condition:

$$\nexists \mathbf{x} \in \mathcal{D} : f_k(\mathbf{x}) < f_k(\mathbf{x}^*),\ \forall k \in \{1,\dots,K\} \tag{21}$$

Assuming that for a given MOOP, the set of Pareto efficient solutions Λ^{P} is compact and not empty, the components of the ideal f_k^{I} and Nadir f_k^{N} $\forall k \in \{1,\dots,K\}$ points are defined correspondingly by the component-wise minimum and maximum of the objective functions vector $f(\mathbf{x})$ for all Pareto efficient solutions $\mathbf{x} \in \Lambda^{\mathrm{P}}$ [39]:

$$f_k^{\mathrm{I}} = \min_{\mathbf{x}\in\Lambda^{\mathrm{P}}} \{f_k(\mathbf{x})\}, \qquad \forall k \in \{1,\dots,K\} \tag{22}$$

$$f_k^{\mathrm{N}} = \max_{\mathbf{x}\in\Lambda^{\mathrm{P}}} \{f_k(\mathbf{x})\}, \qquad \forall k \in \{1,\dots,K\} \tag{23}$$

It is important to note that for conflicting objective functions, the ideal point is not itself a Pareto efficient point, but rather an infeasible theoretical point. Both, the ideal and Nadir points provide relevant information regarding the possible ranges of the objective functions for Pareto efficient solutions, establishing the lower and upper bounds, respectively. The identification of these ranges is crucial for the development of methods of solution for MOO problems, i.e., to construct the set of Pareto efficient solutions. Moreover, with regards to the proposed CP framework, the ideal and Nadir points are the necessary references to design compromise solutions.

3.0.2. Compromise solution(s)

The basic realistic premise of CP is that given a MOOP, any DM seeks optimal solutions as close as possible to the ideal point and/or as far as possible to the Nadir point [40]. To determine such optimal solutions implies the introduction of distance measures, to assess the closeness/farness between points in the objective functions space, and the preferences of the DM. These considerations are commonly addressed in CP by the use of (normalized) weighted ℓ_p norms [41]. Thus, for a given vector of weights $\mathbf{w} = (w_1,\dots,w_k,\dots,w_K)^T$, chosen by the DM and representing the relative importance of each objective function within an MOO context, we can measure the distance (closeness/farness) between the performance provided by any given feasible solution $\mathbf{x} \in \mathcal{D}$ and the ideal and Nadir points by Eqs. (24) and (25), respectively:

$$\ell_p^{\mathrm{I}}(\mathbf{x}) = \left(\sum_{k=1}^{K} w_k^p \left| \frac{f_k(\mathbf{x}) - f_k^{\mathrm{I}}}{f_k^{\mathrm{N}} - f_k^{\mathrm{I}}} \right|^p \right)^{1/p} \tag{24}$$

$$\ell_p^{\mathrm{N}}(\mathbf{x}) = \left(\sum_{k=1}^{K} w_k^p \left| \frac{f_k^{\mathrm{N}} - f_k(\mathbf{x})}{f_k^{\mathrm{N}} - f_k^{\mathrm{I}}} \right|^p \right)^{1/p} \tag{25}$$

Based on the above, it is possible to directly formulate the CP optimization problem (CSP) associated to the given MOOP, whose optimal solution or best-compromise solution is as close as possible to the ideal point and as far as possible to the Nadir point, as presented below:

$$\begin{aligned} \min_{\mathbf{x}} \quad & \ell_p^{\mathrm{I}}(\mathbf{x}) - \ell_p^{\mathrm{N}}(\mathbf{x}) \\ \text{s.t.} \quad & f_k(\mathbf{x}) \le f_k^{\mathrm{N}}, \quad \forall k \in \{1, \dots, K\} \\ & \mathbf{x} \in D \end{aligned} \tag{CSP}$$

It must be noticed that the constraints $f_k(\mathbf{x}) \le f_k^{\mathrm{N}}$, $\forall k \in \{1, \dots, K\}$, are imposed to bound the (CSP), since part of the objective is to find solutions $\mathbf{x}$ that maximize the distances with respect to the Nadir point, but whose performance is better than or 'fall below' the Nadir point.

It has been proved in [39] that the optimal solution $\mathbf{x}^*$ of the problem (CSP) is a Pareto optimal solution of the given MOOP, i.e., $\mathbf{x}^* \in \Lambda^{\mathrm{P}}$, if the ℓ_p norm used to measure distance is *strictly monotone*. In fact, any ℓ_p norm with $1 \le p < \infty$ is *strictly monotone*, guaranteeing Pareto optimality for the purposes here exposed [42]. In this respect, ℓ_1 and ℓ_2 norms, corresponding to the Manhattan and Euclidean distance measures, are among the most commonly used in CP [40], with special attention on the ℓ_1 norm due to the possibility of linearizing the absolute value expressions that define it. Moreover, it is important to mention that the higher the value of p, the more weight is assigned to the largest distances, conditioning the best-compromise solution to be obtained from solving the problem (CSP).

In addition to set the distance metric to use and the relative importance of each objective function, solving the problem (CSP) associated to a given MOOP entails the identification of the ideal and Nadir points. The computation of the ideal point can be easily achieved, whereas, the task of finding the Nadir point is complicated for a MOOP with more than two objective functions. In the following section, we present a practical procedure, based on the work of [39], to compute the ideal and Nadir points for a given MOOP with three objective functions.

3.0.3. Computation of the ideal and Nadir points

In general terms, to determine the ideal point for a MOOP with K objective functions simply require solving K single objective problems of the form $\min_{\mathbf{x}}\{f_k(\mathbf{x}) : \mathbf{x} \in D\}$ for $k \in \{1, \dots, K\}$. This leads directly to obtaining the lower bounds for each objective function and, therefore, the components of the ideal point in the objective functions space, as defined in (22), even if the optimal solutions of these K single objective problems are not all necessarily Pareto efficient solutions of the MOOP, as some of them can result, indeed, weakly Pareto optimal. Given this latter fact, computing the Nadir point from (23), based on the optimal solutions of the mentioned K single objective problems, would lead to an overestimation of it.

The basic idea of the method proposed in [39] is to find a representative subset of Pareto efficient solutions of the MOOP that are sufficient to compute the Nadir point and, complementarily, the ideal point. To explain the method, it is necessary to define the subproblem (MOOP_k), associated to a given MOOP with K objective functions as the same given MOOP but omitting the kth objective function:

$$\begin{aligned} \min_{\mathbf{x}} \quad & (f_1(\mathbf{x}), \dots, f_{k-1}(\mathbf{x}), f_{k+1}(\mathbf{x}), \dots, f_K(\mathbf{x}))^T \\ \text{s.t.} \quad & \mathbf{x} \in D \end{aligned} \tag{MOOP_k}$$

It is worth noting that a MOOP with K objective functions implies K corresponding subproblems (MOOP_k) for $k \in \{1, \dots, K\}$ with $K-1$ objective functions. Then, in all generality, a solution $\mathbf{x}^*$ is called K-Pareto if it is Pareto efficient for the problem (MOOP), i.e., $\mathbf{x}^* \in \Lambda^{\mathrm{P}}$. Moreover, $\mathbf{x}^*$ is called $(K-1)$-Pareto if it is Pareto efficient for any of the K (MOOP_k) subproblems associated to (MOOP), i.e., $\mathbf{x}^* \in \Lambda_k^{\mathrm{P}}$, $k \in \{1, \dots, K\}$.

$(K-1)$-Pareto solutions are necessary to construct the previously mentioned representative subset of Pareto efficient solutions of the problem (MOOP), from which the ideal and Nadir points can be computed, based on the remark that a $(K-1)$-Pareto solution $\mathbf{x}^*$ is either K-Pareto or it is dominated by another K-Pareto solution $\mathbf{x}$ for just one of the K objectives of (MOOP), i.e., $\exists! k' \in \{1, \dots, K\}$ such that $f_{k'}(\mathbf{x}) < f_{k'}(\mathbf{x}^*)$ and $f_k(\mathbf{x}) = f_k(\mathbf{x}^*)$, $\forall k \in \{1, \dots, K\}$ with $k \ne k'$.

Based on the above, the set $\mathcal{O}^{K-1}$, as defined by (26), contains all non-dominated $(K-1)$-Pareto solutions which, at the same time, are K-Pareto solutions or Pareto efficient solutions of the problem (MOOP):

$$\begin{aligned} \mathcal{O}^{K-1} = \{\mathbf{x}^* : \mathbf{x}^* \text{ is } (K-1)\text{-Pareto and } \nexists \mathbf{x} \in \mathcal{O}^{K-1} \\ \text{with } f_k(\mathbf{x}) < f_k(\mathbf{x}^*)\ \forall k \in \{1, \dots, K\}\} \end{aligned} \tag{26}$$

It has been proved in [39] that the set $\mathcal{O}^{K-1}$ contains a subset of solutions that gives the maximum values for each of the K objective functions of the problem (MOOP) for any K-Pareto or Pareto efficient solution, i.e., the Nadir point, and a subset of all global lexicographically optimal solutions of the problem (MOOP) (see Appendix) from which the ideal point can be determined. Then, based on the set $\mathcal{O}^{K-1}$, the ideal and Nadir points can be computed from Eqs. (27) and (28):

$$f_k^{\mathrm{I}} = \min_{\mathbf{x} \in \mathcal{O}^{K-1}} \{f_k(\mathbf{x})\}, \qquad \forall k \in \{1, \dots, K\} \tag{27}$$

$$f_k^{\mathrm{N}} = \max_{\mathbf{x} \in \mathcal{O}^{K-1}} \{f_k(\mathbf{x})\}, \qquad \forall k \in \{1, \dots, K\} \tag{28}$$

A general procedure that summarizes the steps to compute the Nadir and ideal points associated to the K objectives problem (MOOP) is presented in Algorithm 1.

Algorithm 1 Ideal and Nadir points computation

Input: An instance of the problem (MOOP).

1: Set $\mathcal{O}^{K-1} = \emptyset$.
2: **for** $k = 1$ **to** K **do**
3: Determine the set Λ_k^{P} containing the $(K-1)$-Pareto solutions of the problem (MOOP_k).
4: $\mathcal{O}^{K-1} \leftarrow \mathcal{O}^{K-1} \cup \Lambda_k^{\mathrm{P}}$
5: **end for**
6: Remove all dominated solutions from $\mathcal{O}^{K-1}$ as defined in (26).
7: Determine the component-wise minimum and maximum of $f(\mathbf{x}) = (f_1(\mathbf{x}), \dots, f_K(\mathbf{x}))^T$, $\forall \mathbf{x} \in \mathcal{O}^{K-1}$, according to Eqs. (27) and (28), to obtain the ideal f^{I} and Nadir f^{N} points, respectively.

Output: The ideal f^{I} and Nadir f^{N} points, the sets Λ_k^{P}, $\forall k \in \{1, \dots, K\}$.

The procedure of Algorithm 1 requires an embedded method to determine the set of $(K-1)$-Pareto solutions of each problem (MOOP_k) for $k \in \{1, \dots, K\}$. This is practical when computing the Nadir and ideal points of $K = 3$ objectives MOOP, such as the proposed MO two-stage stochastic UC problem, given the broad spectrum of methods available to determine the Pareto efficient solutions of $K - 1 = 2$ objectives problems or, in this case, the 2-Pareto solutions of each problem (MOOP_k) for $k \in \{1, \dots, K\}$. This latter issue is addressed in the following section.

3.0.4. Case with three objectives

The set of 2-Pareto solutions of the two-objective subproblems (MOOP_k), $\forall k \in \{1, \dots, K\}$, associated to the $K = 3$ objectives problem (MOOP), is found by means of the augmented ϵ-constrained method (AUGMECON) [43]. This is a commonly used and effective method for MO mixed integer problems with two objective functions which, to find a Pareto efficient solution, performs the optimization of one objective while restricting the other to the specified value of ϵ. Under this mechanism and the use of an augmented objective function via weighted sum of slack variables, the AUGMECON guarantees the generation of only Pareto efficient solutions [33].

Algorithm 2 presents the procedure to compute N^{P} 2-Pareto efficient solutions for a subproblem (MOOP_k) associated to the problem

Algorithm 2 Computation of 2-Pareto solutions

Input: An instance of the problem (MOOP$_k$), the indexes $k_1, k_2 \in \{1,2,3\}$ of the objectives, with $k_1, k_2 \neq k$, the number of 2-Pareto efficient solutions to determine N^{P} and an adequate small number $\delta \in [10^{-6}, 10^{-3}]$.

1: Set $\Lambda_k^{\mathrm{P}} = \emptyset$.

2: Solve the single objective problems $\min_{\mathbf{x}}\{f_{k_1}(\mathbf{x}) : \mathbf{x} \in \mathcal{D}\}$ and $\min_{\mathbf{x}}\{f_{k_2}(\mathbf{x}) : \mathbf{x} \in \mathcal{D}\}$, determining the solutions $\mathbf{x}^{*f_{k_1}}$ and $\mathbf{x}^{*f_{k_2}}$, respectively.

3: Determine the lexicographically optimal solutions, $\mathbf{x}^{*k_1,k_2}$ and $\mathbf{x}^{*k_2,k_1}$, with respect to the permutations $\pi_1 = (k_1, k_2)$ and $\pi_2 = (k_2, k_1)$, by solving, correspondingly, the following single objective optimization problems:

$$\min_{\mathbf{x}}\{f_{k_2}(\mathbf{x}) : f_{k_1}(\mathbf{x}) \leq f_{k_1}(\mathbf{x}^{*f_{k_1}}), \mathbf{x} \in \mathcal{D}\} \rightarrow \mathbf{x}^{*k_1,k_2}$$

$$\min_{\mathbf{x}}\{f_{k_1}(\mathbf{x}) : f_{k_2}(\mathbf{x}) \leq f_{k_2}(\mathbf{x}^{*f_{k_2}}), \mathbf{x} \in \mathcal{D}\} \rightarrow \mathbf{x}^{*k_2,k_1}$$

4: $\Lambda_k^{\mathrm{P}} \leftarrow \Lambda_k^{\mathrm{P}} \cup \{\mathbf{x}^{*k_1,k_2}, \mathbf{x}^{*k_2,k_1}\}$

5: Set the ideal and Nadir points of the two-objective (MOOP$_k$) problem, respectively, as $f^{\mathrm{I}} = (f_{k_1}(\mathbf{x}^{*k_1,k_2}), f_{k_2}(\mathbf{x}^{*k_2,k_1}))$ and $f^{\mathrm{N}} = (f_{k_1}(\mathbf{x}^{*k_2,k_1}), f_{k_2}(\mathbf{x}^{*k_1,k_2}))$.

6: Compute the ranges of the objective functions as $[f_{k_1}] = f_1^{\mathrm{N}} - f_1^{\mathrm{I}}$ and $[f_{k_2}] = f_2^{\mathrm{N}} - f_2^{\mathrm{I}}$.

7: **for** $i = 3$ **to** N^{P} **do**

8: Sort the set Λ_k^{P} in descending order based on the values of the second objective function $f_{k_2}(\mathbf{x})$, $\forall \mathbf{x} \in \Lambda_k^{\mathrm{P}}$.

9: Compute the normalized (squared) euclidean distances in the objective functions space between consecutive solutions $\mathbf{x}^j$ and $\mathbf{x}^{j+1}$, $\forall j \in \{1, \ldots, |\Lambda_k^{\mathrm{P}}| - 1\}$ with $\mathbf{x}^j, \mathbf{x}^{j+1} \in \Lambda_k^{\mathrm{P}}$:

$$d_{j,j+1}^2 = \left(\frac{f_{k_1}(\mathbf{x}^{j+1}) - f_{k_1}(\mathbf{x}^j)}{[f_{k_1}]}\right)^2 + \left(\frac{f_{k_2}(\mathbf{x}^{j+1}) - f_{k_2}(\mathbf{x}^j)}{[f_{k_2}]}\right)^2, \qquad \forall j \in \{1, \ldots, |\Lambda_k^{\mathrm{P}}| - 1\}, \mathbf{x}^j, \mathbf{x}^{j+1} \in \Lambda_k^{\mathrm{P}}$$

10: Obtain the index associated to the maximum distance $d_{j,j+1}^2$, i.e., $j^* = \underset{j \in \{1,\ldots,|\Lambda_k^{\mathrm{P}}|-1\}}{\operatorname{argmax}} \{d_{j,j+1}^2\}$.

11: Bisect the range of the second objective function, between solutions $\mathbf{x}^{j^*}$ and $\mathbf{x}^{j^*+1}$, by setting the value of ϵ as:

$$\epsilon = f_{k_2}(\mathbf{x}^{j^*+1}) + (f_{k_2}(\mathbf{x}^{j^*}) - f_{k_2}(\mathbf{x}^{j^*+1}))/2$$

12: Solve the following (augmented) ϵ-constrained single objective problem to determine the i-th Pareto efficient solution $\mathbf{x}^i$:

$$\min_{\mathbf{x}}\{f_{k_1}(\mathbf{x}) + \delta\frac{s_{k_2}}{[f_{k_2}]} : f_{k_2}(\mathbf{x}) + s_{k_2} = \epsilon, \mathbf{x} \in \mathcal{D}\} \rightarrow \mathbf{x}^i$$

13: $\Lambda_k^{\mathrm{P}} \leftarrow \Lambda_k^{\mathrm{P}} \cup \{\mathbf{x}^i\}$

14: **end for**

Output: The set Λ_k^{P} of 2-Patero solutions of the problem (MOOP$_k$).

(MOOP), based on the AUGMECON method, and it is composed by two main parts. The first part considers the determination of the ideal and Nadir points of the two-objective subproblem (MOOP$_k$) through lexicographic optimization [39] and the corresponding ranges of the objective functions. The second part of the algorithm regards the resolution of the augmented ϵ-constrained single objective problems for different values of the parameter ϵ. We have integrated a (normalized) euclidean distance-based bisection subroutine to adaptively define the value of ϵ and generate a more equispaced Pareto front.

Having presented the general procedure to compute the Nadir and ideal points of a given MOOP, specifying the embedded method for the case with three objective functions, in the following we explain the process of configuring the (CSP) problem and determining compromise solution(s) of the proposed MO two-stage stochastic UC problem.

The above-mentioned process, presented in Algorithm 3, involves three main stages. The first stage considers the resolution of the single cost-based objective problem for the given instance of the two-stage stochastic UC model. This is done to determine the level of reliability of power supply, measured in terms of total expected load shedding, that the system is able to provide under a traditional cost-based operation scheme that includes the penalty for energy not supplied. Then, an extra constraint is added to the feasible domain of the given instance of the UC problem to ensure that the optimal solution of all optimization (sub)problems, derived from the subsequent stages of the procedure, do not sacrifice reliability of power supply. The second stage involves the identification of the ideal and Nadir points associated to the MO two-stage stochastic UC problem through the application of Algorithm 1 with embedded Algorithm 2. Finally, based on the obtained ideal and Nadir points and a set of vectors of objective functions weights W predefined by the DM, the set of all best-compromise solutions is obtained by solving the corresponding (CSP) problems.

The third stage of Algorithm considers the linearization of the (CSP) problems for the ℓ_1 norm that can be found in Appendix. This to maintain the MILP nature of the deterministic equivalent of all optimization (sub)problems involved in the procedure and to be able to solve them by traditional exact methods.

A crucial issue for the CP framework here proposed concerns the definition by the DM of the weights of the objective functions to determine a specific compromise solution. We recall that these weights establish the preferences of the DM in terms of the relative importance of each objective function within a MOO context. In practice, and for the proposed MO two-stage stochastic UC problem, the DM can certainly have different preferences on the performance regarding the operating costs, CO_2 emissions and wind power curtailment objectives. To define the corresponding weights, the DM can resort to subjective, judgments and expert knowledge, and/or data-driven objective weighting methods within multi-criteria decision-making (MCDM) [44]. In

Algorithm 3 Computation of compromise solution(s) of the MO two-stage UC problem

Input: An instance of the MO two-stage UC problem, the number of 2-Pareto efficient solutions to determine N^{P}, an adequate small number δ, and a set of vectors of weights of the objective functions $W = \{\mathbf{w}^1, \ldots, \mathbf{w}^L\} = \{(w_1^1, w_2^1, w_3^1), \ldots, (w_1^L, w_2^L, w_3^L)\}$.

1: Solve the single cost-based objective UC problem $\min_{\mathbf{x}}\{f_1(\mathbf{x}) : \mathbf{x} \in D\}$ and determine the expected load shedding value associated to the optimal solution:

$$\overline{ELS} = \mathbf{E}(LS^*_{t,\xi}) = \sum_{\xi\in\Omega} \mathbf{P}_\xi \left\{ \sum_{t\in\mathcal{T}} LS^*_{t,\xi} \right\}$$

2: Update the feasible domain of the UC problem, $D \leftarrow D \cap \{\mathbf{E}(LS_{t,\xi}) \le \overline{ELS}\}$.

3: Apply Algorithm 1 (with embedded Algorithm 2) to determine the ideal f^{I} and Nadir f^{N} points and each 2-Pareto solutions set Λ_k^{P}.

4: Set $\Lambda^{\mathrm{C}} = \emptyset$.

5: **for** $l = 1$ **to** L **do**

6: Solve the linearized (CSP) problem (see Appendix) considering the ℓ_1 norm for the objective functions weight vector $\mathbf{w}^l = (w_1^l, w_2^l, w_3^l)$:

$$\min_{\mathbf{x}} \left\{ \sum_{k=1}^{3} w_k^l \frac{|f_k(\mathbf{x}) - f_k^{\mathrm{I}}| - |f_k^{\mathrm{N}} - f_k(\mathbf{x})|}{|f_k^{\mathrm{N}} - f_k^{\mathrm{I}}|} : f_k(\mathbf{x}) \le f_k^{\mathrm{N}}, \forall k \in \{1,2,3\}, \mathbf{x} \in D \right\} \to \mathbf{x}^l$$

7: $\Lambda^{\mathrm{C}} \leftarrow \Lambda^{\mathrm{C}} \cup \{\mathbf{x}^l\}$

8: **end for**

Output: The ideal f^{I} and Nadir f^{N} points, the set Λ_k^{P} of 2-Patero solutions of each (MOOP$_k$) problem with $k \in \{1,2,3\}$, the set Λ^{C} of compromise solutions.

Table 1
Type and technical parameters of conventional power generation units [49–52].

Gen. $g \in \mathcal{G}^{\mathrm{c}}$	Tech.	Energy source	H_g MBtu/MWh	μ_g^{f} ton/MBtu	$\overline{P}_g$ MW	$\underline{P}_g$ MW	$r_g^{\mathrm{U}}, r_g^{\mathrm{D}}$ %	$r_g^{\mathrm{SU}}, r_g^{\mathrm{SD}}$ MW	$t_g^{\mathrm{U}}, t_g^{\mathrm{D}}$ h
1	Hydro	Water	–	–	1040	624	1.000	936	5
2	CST	Coal	8.9	0.096	646	207	0.150	207	3
3	CCGT	Gas	6.6	0.053	725	327	0.300	327	2
4	CST	Coal	8.9	0.096	652	209	0.150	209	3
5	OCGT	Gas	10.0	0.053	508	229	0.500	406	2
6	CST	Coal	8.9	0.096	687	220	0.150	220	3
7	OCGT	Gas	9.6	0.053	580	290	0.500	464	1
8	CST	Coal	8.9	0.096	564	180	0.150	180	3
9	Nuclear	Uranium	9.72	–	865	346	0.050	346	5
10	I.C.[a]	All	8.0	0.077	1100	0	0.325	357	1

[a]Interconnection.

this respect, the analytic hierarchy process (AHP) appears as a practical option that combines quantitative and subjective aspects for determining the weights of multiple objectives by pairwise comparison based on the Saaty's nine-point scale of relative importance [45].

4. Case study

In this section, we present an implementation of the proposed CP framework on a modification of the New England IEEE-39 bus test system [46]. The complete procedure described by Algorithms 1–3 is implemented in Python by programming the involved instances of the proposed two-stage stochastic UC model through the package Pyomo [47], setting Gurobi [48] as MILP solver with optimality gap set to 1%, and run on an Linux machine with Intel® Core™ i7 2.70 GHz and 16 GB of memory.

4.1. System description

The IEEE-39 bus test system presents $|\mathcal{G}| = 10$ conventional generation units, 29 load buses and 46 transmission lines. In the present study, the transmission network is neglected and the aggregated demand of the system is considered for balancing. A diagram of the system is shown in Fig. 1.

The technical parameters by type of technology and cost parameters of conventional power generation units are reported in Tables 1 and 2, respectively.

Table 2
Cost parameters of conventional power generation units [51,52].

Gen. $g \in \mathcal{G}$	C_g^{SU} US$/MW	C_g^{NL} US$/h	C_g^{OM} US$/MWh	C_g^{F} US$/MBtu	C_g^{R} US$/MW
1	0.00	1000	3.4	–	0.00
2	53.50	680	2.97	1.66	1.71
3	37.47	450	3.2	4.68	0.54
4	53.50	680	3.57	1.66	1.71
5	32.12	450	3.5	4.68	0.86
6	53.50	680	2.98	1.66	1.71
7	37.47	480	2.72	4.68	0.86
8	53.50	680	4.5	1.66	1.71
9	25.69	1200	2.3	1.00	0.00
10	0.00	670	5.36	2.44	1.10

The determination of the best-compromise Pareto efficient on/off schedules is performed for an horizon of $\mathcal{T} = 24$ h with hourly resolution $\Delta t = 1$ h. Within this horizon, the mean μ_t MW values of the hourly normally distributed aggregated demand profile are reported in Table 3 and the corresponding hourly standard deviation σ_t MW values are considered as the 10% of the hourly mean values.

Regarding wind power generation, a single wind farm is considered in the system to accentuate the effects of wind power variability. The farm ensures a rated capacity of 2500 MW, consisting on $N_g^{\mathrm{W}} = 1250$ wind turbines with $P_g^{\mathrm{R}} = 2$ MW of rated power based on the Vestas V90 model [53]. The respective cut-in, rated and cut-out wind speeds

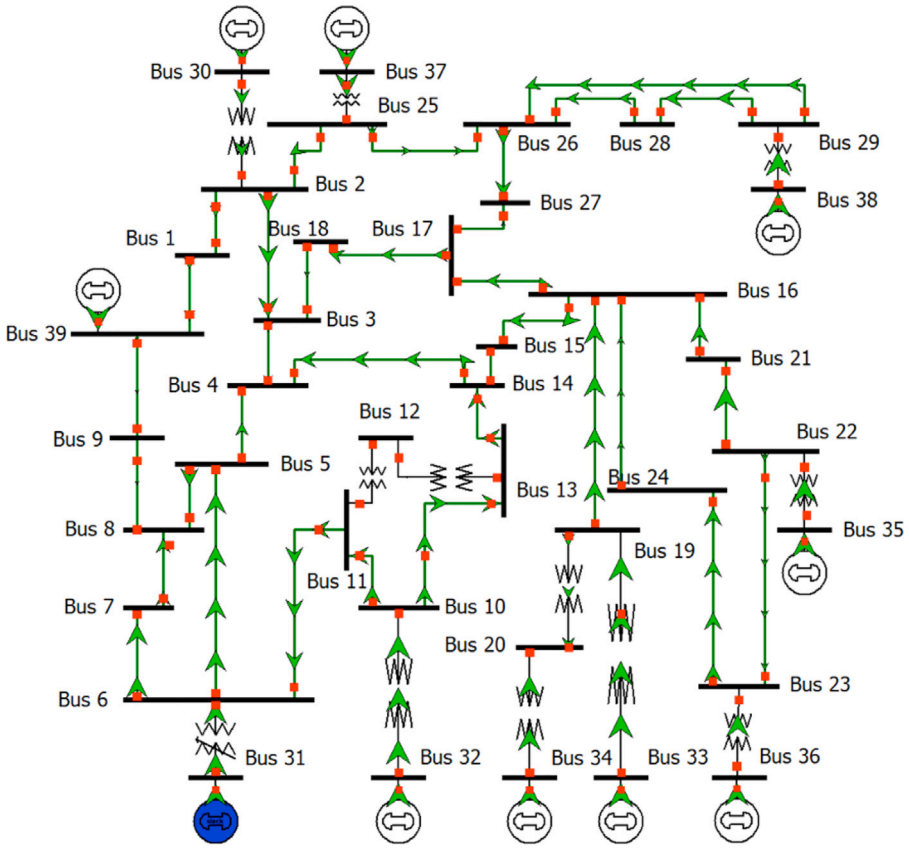

Fig. 1. Diagram of the New England IEEE 10 generators 39-Bus test system.

Table 3
Mean values of the hourly aggregated demand profile [51,52].

$t \in \mathcal{T}$	μ_t (MW)	$t \in \mathcal{T}$	μ_t (MW)
1	2139.12	13	4278.25
2	2291.92	14	3972.66
3	2597.51	15	3667.07
4	2903.10	16	3208.68
5	3055.89	17	3055.89
6	3361.48	18	3361.48
7	3514.27	19	3667.07
8	3667.07	20	4278.25
9	3972.66	21	3972.66
10	4278.25	22	3361.48
11	4431.04	23	2750.30
12	4583.84	24	2444.71

for the wind energy conversion model (21) are $U_g^{\text{in}} = 4$ m/s, $U_g^{\text{R}} = 13$ m/s and $U_g^{\text{out}} = 25$ m/s. The hub height of the wind turbines is 80 m. In addition, as presented in Section 2, a Matérn process-based model is used to simulate the hourly wind speed series profiles for the scheduling horizon. For this, the parameters of the model are obtained through a fitting process performed on an annual wind speed time series with 30 min resolution measured at 53 m, corresponding to the Megler site for meteorological observations, which forms part of the Bonneville Power Administration (BPA) [54]. Then, the fitted parameters, that characterize the amplitudes, frequencies and phases of high-energy periodic components in the mean and variance of the annual wind speed data series and the underlying random component (Matérn process), are delivered as inputs to a simulation procedure that allows to compose synthetic wind speed series from white Gaussian noise. More details on the fitting process, fitted parameters and the simulation procedure can be found in [36].

Considering the above, we generate random wind speed time series with hourly resolution and 24 h size, corresponding arbitrarily to the second day of February. Moreover, we extrapolate the simulated wind speed time series at the hub height of the wind turbines by means of a Hellman power law model with an average day-night wind shear exponent $\alpha^{\text{H}} = 0.32$ [55]. In this manner, the simulated wind speed profiles present a Weibull-like distribution with approximated shape and scale parameters $k = 2.088$ and $a = 8.596$, and a daily average of 7.602 m/s, implying an average wind energy penetration of approx. 32%.

Additional parameters include the variable O&M cost associated to the wind farm $C_g^{\text{OM}} = 5$ US$/MWh [56], the penalty cost for energy not supplied $C^{\text{ENS}} = 10000$ US$/MWh and the systemic spinning reserve requirements set as $r^{\min} = 3\%$ of the aggregated demand for each hour within the scheduling horizon [20].

4.2. Representative scenarios

It is well known that the computational burden from the stochastic formulations of the UC problem increases exponentially with the number of scenarios considered [57]. To be able to solve all instances of the two-stage stochastic UC model within the proposed CP framework in reasonable computational times, we implement a scenario-reduction technique based on the unsupervised k-means clustering method [58]. For this, we generate a set of $|\Omega'| = 500$ scenarios composed by discrete time series for the available wind power $\{P^{\text{W}}_{g,t,\xi}\}_{t=1,\ldots,|\mathcal{T}|}$ at the wind farm (that depends on the sampled wind speed time series $\{ws_{g,t,\xi}\}_{t=1,\ldots,|\mathcal{T}|}$ according to (21)) and the aggregated demand $\{D_{t,\xi}\}_{t=1,\ldots,|\mathcal{T}|}$, with $\xi \in \Omega'$, on which the k-means technique is applied. By doing this, k clusters of days with similar operational conditions are determined based on the minimization of the within-cluster sum of squares. In this work, it has been empirically found, by solving

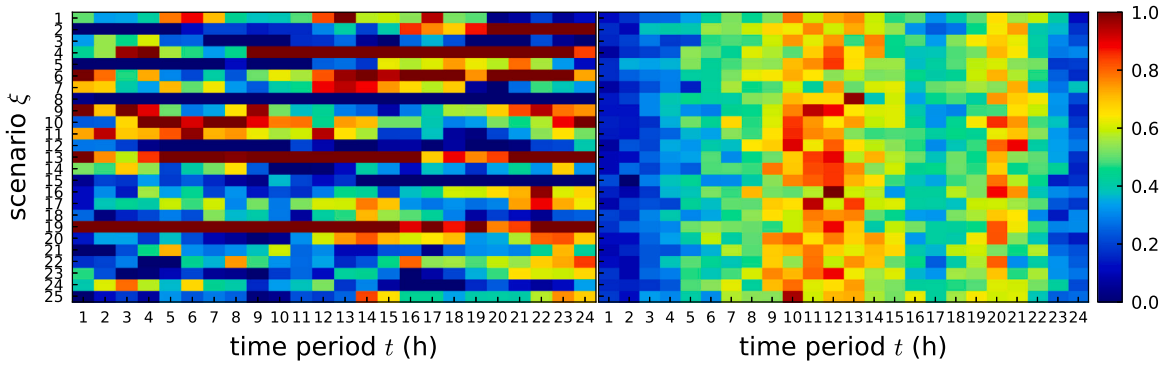

Fig. 2. Representative scenarios. Scaled available wind power (left) and aggregated demand (right).

Table 4
Representative scenarios probability of occurrence.

$\xi \in \Omega$	$\mathbf{P}_\xi$	$\xi \in \Omega$	$\mathbf{P}_\xi$
1	0.046	14	0.030
2	0.030	15	0.020
3	0.018	16	0.040
4	0.030	17	0.036
5	0.026	18	0.050
6	0.072	19	0.020
7	0.074	20	0.052
8	0.016	21	0.122
9	0.034	22	0.016
10	0.028	23	0.026
11	0.036	24	0.066
12	0.046	25	0.026
13	0.040	–	–

Table 5
Set W of objective functions weights vectors for best-compromise solutions design.

Case	W	$\mathbf{E}(C_\xi^{\mathrm{T}})$	$\mathbf{E}(E_\xi^{\mathrm{TCO_2}})$	$\mathbf{E}(PC_\xi^{\mathrm{TW}})$
(i)	$\mathbf{w}^1$	0.333	0.333	0.333
(ii)	$\mathbf{w}^2$	0.400	0.400	0.200
(iii)	$\mathbf{w}^3$	0.571	0.286	0.143
(iv)	$\mathbf{w}^4$	0.286	0.571	0.143

the three single objective two-stage stochastic UC problem for each proposed objective function, that the optimal values begin to stabilize for $|\Omega| = 20$ scenarios. Consequently, a number of $k = 25$ has been set in the k-means algorithm to obtain a set of $|\Omega| = 25$ representative scenarios for the available wind power at the wind farm and the aggregated demand. These representative scenarios correspond to the sampled series $\{P^{\mathrm{W}}_{g,t,\xi}\}_{t=1,\ldots,|\mathcal{T}|}$ and $\{D_{t,\xi}\}_{t=1,\ldots,|\mathcal{T}|}$, with $\xi \in \Omega'$, which are the closest, according to the euclidean distance, to the centroid of each cluster. The probability of occurrence of each representative scenario $\mathbf{P}_\xi$, $\forall \xi \in \Omega$, is approximated as the number of scenarios per cluster over the number of sampled scenarios $|\Omega'| = 500$. Fig. 2 shows the scaled values for the available wind power $\{P^{\mathrm{W}}_{g,t,\xi}\}_{t=1,\ldots,|\mathcal{T}|} \in [0, 2500]$ MW and aggregated demand $\{D_{t,\xi}\}_{t=1,\ldots,|\mathcal{T}|} \in [1595.88, 5518.25]$ MW for the representative scenarios $\xi \in \Omega$, whereas the corresponding probabilities $\mathbf{P}_\xi$, $\forall \xi \in \Omega$ are presented in Table 4.

4.3. Compromise solutions design

The DM's preferences, represented by the set of vectors of weights of the objective functions $W = \{\mathbf{w}^1, \ldots, \mathbf{w}^L\}$ in the proposed CP framework, are introduced to design best-compromise on/off schedules that balance operating cost, CO_2 emissions and wind power curtailment performance in accordance to the relative importance between these three objectives. In this work, we aim at the design of best-compromise on/off schedules in four different cases, based on theoretical and realistic considerations:

Table 6
Summary of optimal solutions.

Solution		$\mathbf{E}(C_\xi^{\mathrm{T}})$ (kUS$)	$\mathbf{E}(E_\xi^{\mathrm{TCO_2}})$ (Mton)	$\mathbf{E}(PC_\xi^{\mathrm{TW}})$ (MW)
min. $\mathbf{E}(C_\xi^{\mathrm{T}})$	–	1390.37	25732.36	10635.12
$\in \Lambda_3^{\mathrm{P}}$	$\in \mathcal{O}^2$	1390.37	25722.13	10626.11
$\in \Lambda_3^{\mathrm{P}}$	$\in \mathcal{O}^2$	1402.16	22334.59	11293.79
$\in \Lambda_3^{\mathrm{P}}$	$\in \mathcal{O}^2$	1415.92	18947.05	11171.47
$\in \Lambda_3^{\mathrm{P}}$	$\in \mathcal{O}^2$	1462.96	17425.30	10591.98
$\in \Lambda_3^{\mathrm{P}}$	$\in \mathcal{O}^2$	1495.12	15903.54	10525.45
$\in \Lambda_3^{\mathrm{P}}$	$\in \mathcal{O}^2$	1554.85	14381.78	10530.02
$\in \Lambda_3^{\mathrm{P}}$	$\in \mathcal{O}^2$	1599.98	13620.90	10542.16
$\in \Lambda_3^{\mathrm{P}}$	$\in \mathcal{O}^2$	1635.75	13240.46	9957.33
$\in \Lambda_3^{\mathrm{P}}$	$\in \mathcal{O}^2$	1704.45	12860.03	10037.58
min. $\mathbf{E}(E_\xi^{\mathrm{TCO_2}})$	–	1716.23	12860.02	6419.54
min. $\mathbf{E}(C_\xi^{\mathrm{T}})$	–	1390.37	25732.36	10635.12
$\in \Lambda_2^{\mathrm{P}}$	$\in \mathcal{O}^2$	1390.37	25722.13	10626.05
$\in \Lambda_2^{\mathrm{P}}$	$\in \mathcal{O}^2$	1392.60	25707.09	9143.43
$\in \Lambda_2^{\mathrm{P}}$	$\in \mathcal{O}^2$	1394.97	25707.09	7660.81
$\in \Lambda_2^{\mathrm{P}}$	$\in \mathcal{O}^2$	1397.35	25707.09	6178.19
$\in \Lambda_2^{\mathrm{P}}$	$\in \mathcal{O}^2$	1426.11	28458.85	4696.00
$\in \Lambda_2^{\mathrm{P}}$	$\in \mathcal{O}^2$	1488.21	28807.65	3920.03
$\in \Lambda_2^{\mathrm{P}}$	$\in \mathcal{O}^2$	1534.66	29699.18	3531.87
$\in \Lambda_2^{\mathrm{P}}$	$\in \mathcal{O}^2$	1587.88	28941.65	3337.28
$\in \Lambda_2^{\mathrm{P}}$	$\in \mathcal{O}^2$	1714.58	29298.73	3142.45
min. $\mathbf{E}(PC_\xi^{\mathrm{TW}})$	–	1807.80	28545.40	3142.45
min. $\mathbf{E}(PC_\xi^{\mathrm{TW}})$	–	1807.80	28545.40	3142.45
$\in \Lambda_1^{\mathrm{P}}$	$\in \mathcal{O}^2$	1830.85	26878.64	3142.45
$\in \Lambda_1^{\mathrm{P}}$	$\in \mathcal{O}^2$	1945.40	23721.25	3247.93
$\in \Lambda_1^{\mathrm{P}}$	$\in \mathcal{O}^2$	1885.94	20563.85	3566.64
$\in \Lambda_1^{\mathrm{P}}$	$\in \mathcal{O}^2$	1815.77	17406.46	3791.10
$\in \Lambda_1^{\mathrm{P}}$	$\in \mathcal{O}^2$	1792.85	14249.06	4109.92
$\in \Lambda_1^{\mathrm{P}}$	$\in \mathcal{O}^2$	1724.90	13554.54	4374.04
$\in \Lambda_1^{\mathrm{P}}$	$\in \mathcal{O}^2$	1715.90	13207.28	4611.62
$\in \Lambda_1^{\mathrm{P}}$	$\in \mathcal{O}^2$	1719.24	13033.65	4869.61
$\in \Lambda_1^{\mathrm{P}}$	$\in \mathcal{O}^2$	1715.17	12860.03	5492.31
min. $\mathbf{E}(E_\xi^{\mathrm{TCO_2}})$	–	1716.23	12860.02	6419.54
Ideal point		1390.37	12860.02	3142.45
Nadir point		1945.40	29699.18	11293.79

Table 7
Summary of designed best-compromise solutions.

Solution		$\mathbf{E}(C_\xi^{\mathrm{T}})$ (kUS$)	$\mathbf{E}(E_\xi^{\mathrm{TCO_2}})$ (Mton)	$\mathbf{E}(PC_\xi^{\mathrm{TW}})$ (MW)	d^1	d^{N}
Case (i)	$\mathbf{w}^1$	1571.21	15346.04	4979.73	0.699	2.301
Case (ii)	$\mathbf{w}^2$	1514.69	16044.15	5109.95	0.654	2.346
Case (iii)	$\mathbf{w}^3$	1429.57	20329.23	5972.59	0.861	2.139
Case (iv)	$\mathbf{w}^4$	1682.28	14848.81	5555.23	0.940	2.060

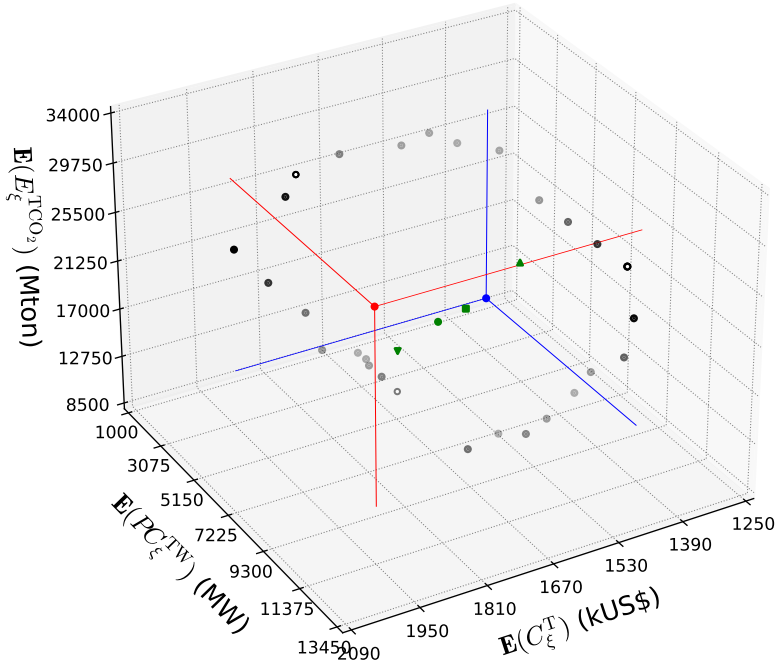

Fig. 3. 3D representation of the obtained 3-Pareto efficient and best-compromise solutions.

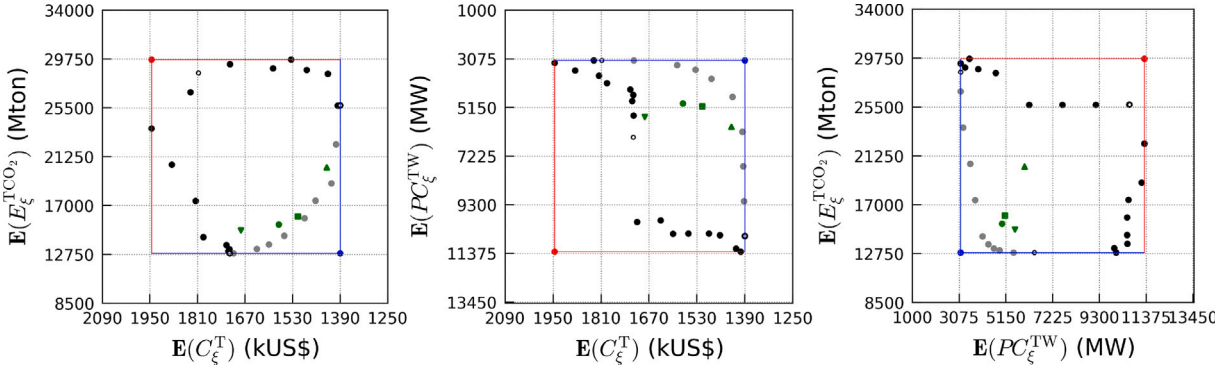

Fig. 4. 2D projections of the obtained 3-Pareto efficient and best-compromise solutions.

(i) The three objective functions are equally important.
(ii) Operating cost and CO_2 emissions performance are equally important, and both are twice as important as wind power curtailment performance.
(iii) Operating cost performance is twice as important as CO_2 emissions performance, and the latter is twice as important as wind power curtailment performance.
(iv) CO_2 emissions performance is twice as important as Operating cost performance, and the latter is twice as important as wind power curtailment performance.

As it can be inferred from above, case (i) considers the design of a best-compromise on/off schedule for which the three objectives are equally important. This solution will provide a reference for comparison, but does not necessarily represent the DM's preferences in reality. For this reason, we formulate the Cases (ii), (iii) and (iv) for which we search for best-compromise on/off schedules focusing on a more intense trade-off between economic and environmental performance, but without disregarding the potential benefits of diminishing wind power curtailment.

The relative importance between the objectives for all aforementioned cases of design of best-compromise on/off schedules have been defined based on the Saaty's universal nine-point scale, used as part of the AHP method [45]. Then, the vector of objective function weights $\mathbf{w}^l$ for each case $l \in \{1,\dots,4\}$ can be easily determined from each judgment matrix metric resulting from the corresponding comparison between rated objectives. The weights $\mathbf{w}^l$ for each case $l \in \{1,\dots,4\}$ are reported in Table 5.

4.4. Results and discussion

The results are presented in accordance to the steps of the Algorithm 3 that summarizes the proposed framework. Thus, by applying the first stage of the algorithm (steps 1 to 3), we determine an expected load shedding value $\mathbf{E}(LS^*_{t,\xi}) = 7.252$ MW by solving the single cost-based objective UC problem and updating the domain of all subsequent (sub)problems so as all Pareto optimal solutions to be found present at least that level of reliability of power supply. It must be pointed out that 7.252 MW of expected load shedding represents the 0.009% of the total expected load of 82814 MW within the scheduling horizon, i.e., it is practically negligible. In addition, the first stage of Algorithm 3 considers the application of Algorithm 1 with the embedded procedure of Algorithm 2 to determine the sets Λ_k^{P} containing $N^{\mathrm{P}} = 9$ 2-Pareto solutions associated to each two-objective (MOOP_k) with $k \in \{1,2,3\}$ and compute the corresponding Ideal and Nadir points. A summary of the objective function values associated to all optimal solutions

Table 8
Percentage variation of objective functions of best-compromise schedules.

Solution		$\Delta_{\%}\mathbf{E}(C_\xi^{\mathrm{T}})$	$\Delta_{\%}\mathbf{E}(E_\xi^{\mathrm{TCO_2}})$	$\Delta_{\%}\mathbf{E}(PC_\xi^{\mathrm{TW}})$
Case (i)	$\mathbf{w}^1$	13.01	−40.36	−53.18
Case (ii)	$\mathbf{w}^2$	8.94	−37.65	−51.95
Case (iii)	$\mathbf{w}^3$	2.82	−21.00	−43.84
Case (iv)	$\mathbf{w}^4$	21.00	−42.30	−47.77

Table 9
Shadow prices derived from the best-compromise solutions.

Solution		$\lambda_{\mathbf{E}(E_\xi^{\mathrm{TCO_2}})}$ (US$/Mton)	$\lambda_{\mathbf{E}(PC_\xi^{\mathrm{TW}})}$ (US$/MW)
Case (i)	$\mathbf{w}^1$	32.48	68.27
Case (ii)	$\mathbf{w}^2$	32.53	30.54
Case (iii)	$\mathbf{w}^3$	16.93	17.37
Case (iv)	$\mathbf{w}^4$	36.69	20.34

Table 10
Expected operating cost break down. All quantities expressed in kUS$.

Solution		$\mathbf{E}(C_\xi^{\mathrm{SU}})$	$\mathbf{E}(C_\xi^{\mathrm{NL}})$	$\mathbf{E}(C_\xi^{\mathrm{OM}})$	$\mathbf{E}(C_\xi^{\mathrm{F}})$	$\mathbf{E}(C_\xi^{\mathrm{R}})$	$\mathbf{E}(C_\xi^{\mathrm{ENS}})$
min. $\mathbf{E}(C_\xi^{\mathrm{T}})$	–	229.28	108.00	298.16	670.76	11.65	72.52
Case (i)	$\mathbf{w}^1$	218.53	83.60	306.77	880.65	9.71	71.94
Case (ii)	$\mathbf{w}^2$	206.86	86.00	314.19	825.86	9.59	72.18
Case (iii)	$\mathbf{w}^3$	241.42	100.46	308.21	718.36	11.46	49.66
Case (iv)	$\mathbf{w}^4$	319.77	84.51	303.20	895.71	11.82	67.28

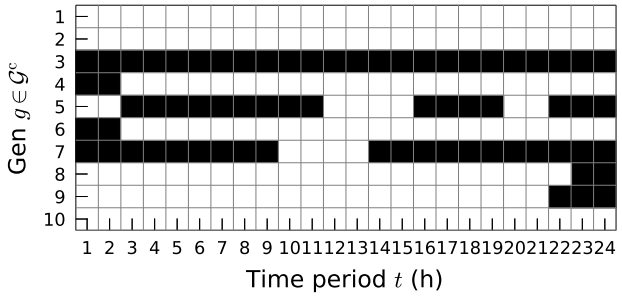

Fig. 5. Optimal min. $\mathbf{E}(C_\xi^{\mathrm{T}})$ on/off schedule.

obtained in this process is reported in Table 6; the optimal solutions denoted min. $\mathbf{E}(C_\xi^{\mathrm{T}})$, min. $\mathbf{E}(E_\xi^{\mathrm{TCO_2}})$ and min. $\mathbf{E}(PC_\xi^{\mathrm{TW}})$ are obtained by minimizing each objective function individually.

It is worth noticing that all the 2-Pareto solutions obtained are, in fact, 3-Pareto solutions, i.e., they are Pareto efficient solutions of the proposed three-objectives two stage stochastic UC problem. According to this, they all compose the representative subset $\mathcal{O}^2$ of Pareto efficient solutions from which the ideal and Nadir points are computed.

In regards to the designed best-compromise solutions, through the application of the second stage of Algorithm 3, we obtain the Pareto efficient solutions corresponding to the four cases formulated in accordance to the established DM's preferences. Table 7 presents the objective function values associated to the designed four best-compromise solutions and the corresponding distances, measured through the ℓ_1 norm, to the ideal and Nadir points.

From Table 7, it can be noticed that the optimal values of the three objective functions obtained for the best-compromised solutions are coherent to the assigned relative importance (weight) in each case, i.e., the higher the relative importance of the objective function, the lower the corresponding optimal value provided by the respective schedule. Furthermore, under the basic realistic premise of CP, the optimal schedules obtained for case (i) and, especially, for case (ii) are interesting solutions since they are comparatively closer to the ideal point and farther from the Nadir point. Notwithstanding the foregoing, the optimal schedules obtained for cases (iii) and (iv) can also be interesting for the DM, given their respective proximity to the schedules that individually minimize operating cost and CO_2 emissions performance.

The above mentioned insights are observable in Figs. 3 and 4 which show, respectively, a 3D representation of the obtained 3-Pareto efficient and best-compromise solutions and their 2D projections onto three of the planes formed by pairs of the three objective functions. The optimal solutions that individually minimize operating cost, CO_2 emissions and wind power curtailment performance, i.e., min. $\mathbf{E}(C_\xi^{\mathrm{T}})$, min. $\mathbf{E}(E_\xi^{\mathrm{TCO_2}})$ and min. $\mathbf{E}(PC_\xi^{\mathrm{TW}})$, respectively, are depicted as white bullets with black border, whereas bullets in shades of gray represent 3-Pareto solutions belonging to the $\mathcal{O}^2$ set. The obtained best-compromised solutions are colored in green and differentiated by markers: case (i) - bullet, case (ii) - square, case (iii) - up triangle and case (iv) - down triangle. Ideal and Nadir points are represented correspondingly by blue and red bullets.

From hereafter, a comparative analysis is performed, regarding the operational performance of the obtained best-compromise schedules against the minimal cost schedule, i.e., min. $\mathbf{E}(C_\xi^{\mathrm{T}})$, which is the solution provided by the traditional approach of addressing the UC problem.

Table 8 reports the percentage variation of the optimal objective function values associated to the best-compromise schedules with respect to the minimum cost schedule. As it can be inferred for all best-compromise schedules, significant simultaneous reductions can be achieved in CO_2 emissions and wind power curtailment performance by conservatively sacrificing operating cost. Evidently, the selection of an optimal schedule by the DM depends on its preferences on the objectives. For instance, the minimum cost solution, min. $\mathbf{E}(C_\xi^{\mathrm{T}})$, subscribes 10635 MW of expected wind power curtailment, meaning an average rate of 41.32% of discarded wind energy within the planning horizon, rate that lies far outside the acceptable range of 5%–20% of wind energy curtailment to maintain an efficient and stable operation [59,60]. The wind energy curtailment rates associated to the obtained best-compromise schedules are 19.34%, 19.85%, 23.20% and 21.58% for cases (i) to (iv), respectively, suggesting that the DM should consider schedules (i) or (ii) to comply with a tolerable level of wind energy curtailment. Then, the selection between these two solutions will lie in the trade-off between operational cost and CO_2 emissions performance. If such is the case, best-compromise schedule (ii) presents a greater percentage reduction of CO_2 emission levels by percentage point of operational cost increment, a fact that is coherent with the proximity and farness of this solution to the ideal and from the Nadir points, respectively.

Moreover, each obtained best-compromised solution can be interpreted as an optimal solution coming from a single objective model that minimizes (expected) total operating cost including cost penalties associated to CO_2 emissions and wind power curtailment. Indeed, these cost penalties can be estimated, and not arbitrarily defined, through duality theory by giving in input the fixed values of the first stage binary decision variables of each best-compromised solution to the continuous linear program corresponding to the second stage of decisions of the proposed stochastic UC model, including two additional constraints associated to the expected values of the total CO_2 emissions and wind power curtailment, $\mathbf{E}(E_\xi^{\mathrm{TCO_2}})$ Mton and $\mathbf{E}(PC_\xi^{\mathrm{TW}})$ MW, respectively. By solving the dual associated to the second stage problem for each case, we can estimate the shadow prices, $\lambda_{\mathbf{E}(E_\xi^{\mathrm{TCO_2}})}$ US$/Mton and $\lambda_{\mathbf{E}(PC_\xi^{\mathrm{TW}})}$ US$/MW corresponding to the mentioned constraints. The values of the shadow prices (cost penalties) estimated in this manner are reported in Table 9. As it can be seen, the values obtained for the shadow prices in each case are coherent with the intensity of variations achieved for the optimal objective function values for CO_2 and wind power curtailment performance.

In regards to the optimal schedules provided by the solutions under analysis, Figs. 5 and 6 present the behavior of the on/off status variables within the scheduling horizon for the conventional generation

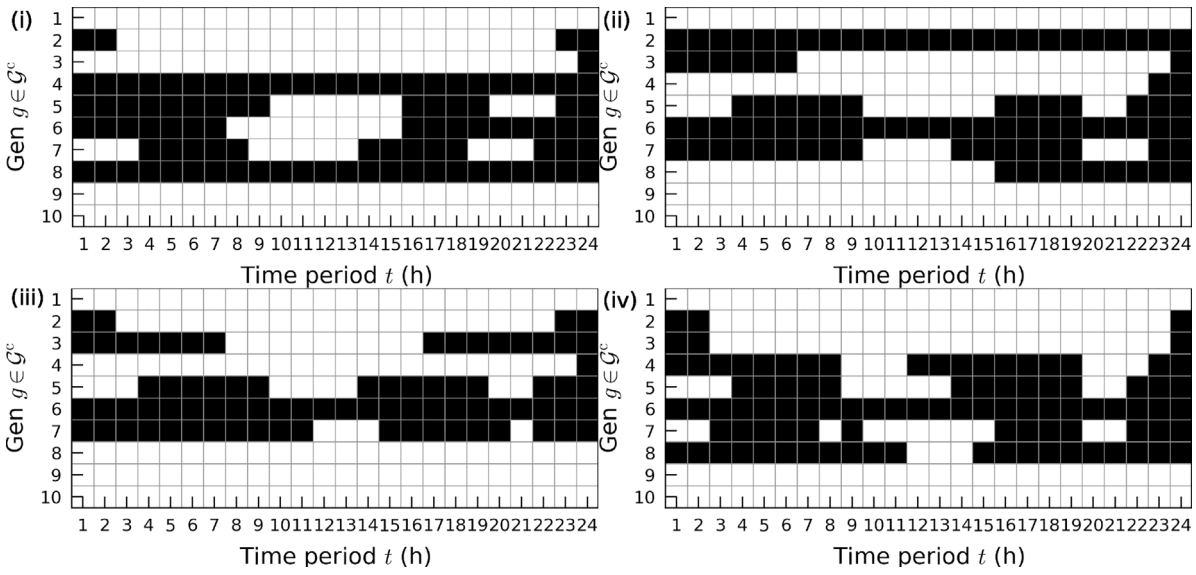

Fig. 6. Best-compromise on/off schedules.

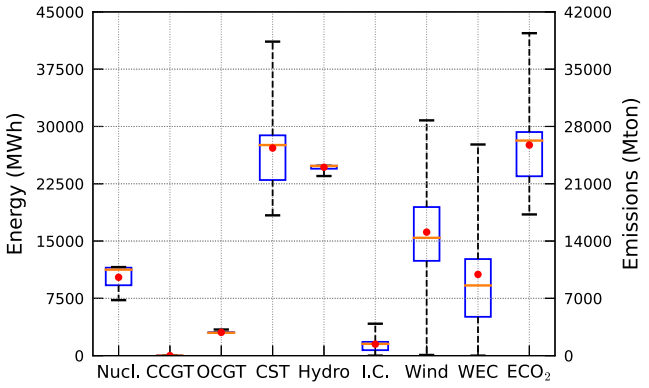

Fig. 7. Total energy production by technology, wind energy curtailment and CO_2 within the scheduling horizon. Optimal min. $\mathbf{E}(C_\xi^{\mathrm{T}})$ solution.

units for the minimum cost and the best-compromise solutions, respectively, white and black cells indicating correspondingly on, $x_{g,t} = 1$, and off, $x_{g,t} = 0$, statuses with $g \in \mathcal{G}^c, t \in \mathcal{T}$. As it can be observed in both Figures, all optimal schedules are coherent with the mean profile of the aggregated demand of power, i.e., more generators are in on status during the peak demand intervals between 9–14 h and 19–22 h, and in off status during low demand hours. However, the reliance on the type of generation technologies differs among these optimal solutions. On the one hand, the minimum cost schedule, min. $\mathbf{E}(C_\xi^{\mathrm{T}})$, relies strongly on coal-based CST ($g = 2, 4, 6, 8$), Hydro ($g = 1$) and Nuclear ($g = 9$) technologies, in addition to the interconnection I.C. ($g = 10$), and in a lesser degree on the gas-based OCGT ($g = 5, 7$). Moreover, this optimal schedule shows in general a low cycling frequency with the exception of the OCGT generation units. On the other hand, the optimal schedules provided by the best-compromised solutions, although they show the same reliance on Hydro and Nuclear technologies and the I.C., they differ with respect to the min. $\mathbf{E}(C_\xi^{\mathrm{T}})$ schedule in how the thermal units are cycled and the frequency of cycling. For instance, the schedule of the best-compromise solutions (i), for which all objectives have the same importance for the DM, gas-based CCGT ($g = 3$) is on status practically throughout all the scheduling horizon and gas-based OCGT ($g = 5, 7$) cycle conjointly more frequently. This is an evidence of trading off the use of cheaper coal-based generation units ($g = 4, 8$) and the use of more expensive and flexible gas-based generation that allows improving CO_2 emissions and wind power curtailment performance. This same trade-off pattern is observable in optimal schedules (ii), (iii) and (iv), but varying according the DM's preferences and noticeable by the use of the coal-based generation units. To better explain this use, we resort to Figs. 7 and 8 which present weighted box plots, based on the $|\Omega| = 25$ representative scenarios and their probabilities of occurrence $\mathbf{P}_\xi$, of the total energy production of each generation technology and wind energy curtailment (WEC) (left y-axis), and the total production of CO_2 emissions within the scheduling horizon (right y-axis) associated to the minimum cost and best-compromise schedules, respectively. The boxes and whiskers of the box plots represent the values within the ranges defined correspondingly by the 25-75th and 1-99th percentiles, whereas the median and mean values are depicted as orange line and red bullet, respectively.

Fig. 7 shows an intensive reliance of the optimal schedule min. $\mathbf{E}(C_\xi^{\mathrm{T}})$ on the coal-based CST generation units. Indeed, this schedule is cost-effective because it profits mostly from the comparatively low O&M and fuel costs of this technology (see Table 10) but at the expense of increasing CO_2. Moreover, even though technologies such as Hydro and Nuclear contribute to satisfy the demand, their accumulated energy output within the planning seems to be stable within the planning horizon and across all scenarios. Conversely, the total output of coal-based CST generation units presents more variability, indicating that this technology accommodates to the variability in the aggregated power demand and contributes with its limited ramping rate to the integration of restricted amounts of wind energy. Different is the case of best-compromise solutions (i) and (ii) (Fig. 8) for which CO_2 emissions and wind power curtailment enter the objectives trade-off with considerable relative importance. In both cases, a significant decrease is observable in the use of coal-based CST technology, being replaced by the use of less polluting gas-based CCGT and OCGT technologies and the I.C., allowing to reduce CO_2 emissions. Nevertheless, the consequence of this exchange in generation technologies increases the expected O&M and fuel costs in optimal schedules (i) and (ii) (see Table 10). Moreover, for these schedules, the total energy output within the scheduling horizon of Nuclear, CCGT, OCGT, Hydro and the I.C. presents more dispersion, indicating their contribution with ramping to accommodate the variability of the power demand and wind power, a fact that is supported by the reduced levels of wind energy curtailment (WEC) provided by these solutions.

Continuing with the above, best-compromise solutions (iii) and (iv) (Fig. 8) present similar characteristic to those exposed for the cases (i) and (ii). Recalling that, for the design of the best compromise (iii),

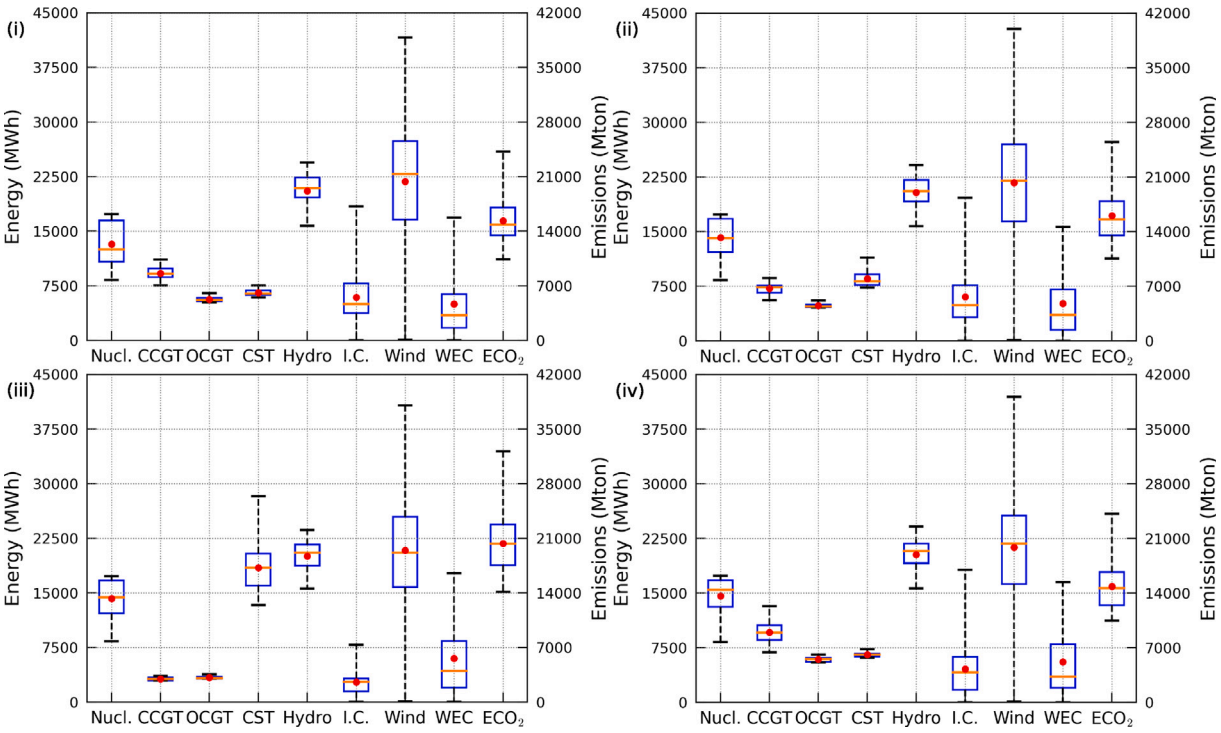

Fig. 8. Total energy production by technology, wind energy curtailment and CO_2 within the scheduling horizon. Best-compromise solutions.

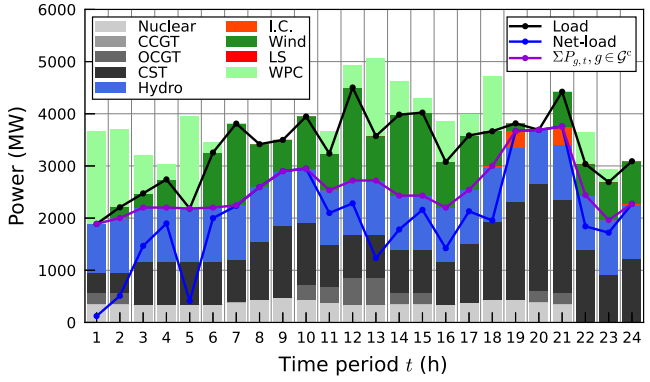

Fig. 9. Aggregated power dispatching by generation technology. Representative scenario $\xi = 7$. Optimal min. $\mathbf{E}(C^{\mathrm{T}}_{\xi})$ solution.

the relative importance of operating costs is the highest, the solution shows an increased participation of the coal-based CST technology, but in a lower degree with respect to the cost-effective solution min. $\mathbf{E}(C^{\mathrm{T}}_{\xi})$, since CO_2 emissions performance is also in the trade-off of objectives as the second most important one. In addition, the energy output of cleaner technologies such as Nuclear, Hydro and the I.C. show some degree of dispersion, explaining the more conservative reduction of WEC with respect to solutions (i) and (ii). Contrastingly, best-compromise solutions (iv) which prioritizes CO_2 emissions performance, relies to a higher extent on gas-based CCGT technology, when compared to solution (iii), and on the cycling of gas-based OCGT unit $g = 7$ and the ramping of the I.C. to provide additional flexibility to integrated wind energy. It is worth noting in Table 10 that best-compromise solution (iv) subscribes a most significant start-up costs component.

The above insights can be complemented by analyzing the power dispatch by generation technology for the minimum cost and best-compromise solutions for a representative operational scenario with a high probability of occurrence and high level of wind energy availability, shown in Figs. 9 and 11. The scenario under consideration is $\xi = 7$ which presents 30715 MWh of available wind energy within the planning horizon, meaning a 51% of the full capacity of the wind farm. For this scenario, the minimum cost and best-compromise solutions, from (i) to (iv), subscribe a wind energy curtailment rate of 41.16%, 20.15%, 22.84%, 27.19% and 25.91%, respectively.

As it can be seen in Fig. 9, the dispatching decisions for scenario $\xi = 7$ for the minimum cost schedule show a stable behavior of the Hydro technology which operates practically at maximum capacity throughout all the scheduling horizon. This is due to the comparatively low variable O&M cost associated to this technology. Further, it is also noticeable the aggregated operating cost-effective contribution of coal-based CST technology to satisfy demand, which also provides ramping of its power output to accommodate wind power which is, in turn, cost-effective. Nevertheless, the flexibility provided by the schedule, by cycling and ramping mainly the thermal units, it is not sufficient to properly cope with the ramp requirements imposed by the net-load, or demand-less available wind power, evidenced as mismatches between the curve of aggregated power output of conventional technologies (purple) and the net-load curve (blue). Any mismatch between these two curves throughout the scheduling horizon implies incurring in wind power curtailment, given the priority to avoid load-shedding. In this view, although this schedule is cost-effective, it presents limited CO_2 emissions and wind power curtailment performance, since it resorts primarily to coal-based CST technology for flexibility, whose ramping capability is restricted. Even though the current analysis is performed considering solely the representative scenario $\xi = 7$, this dispatching decision pattern is consistent for all scenarios. Indeed, these same insights are coherent with what exposed in Fig. 11 that presents the weighted box plot, based on all representative scenarios, of the hourly power production of each conventional generation technology within the scheduling horizon for the minimum cost schedule.

With regards to the dispatching decisions for scenario $\xi = 7$ for best-compromised solutions, it can be seen in Fig. 10 that in all cases, all conventional generation technologies and the I.C. provide ramping, to different extents depending on the DM's preferences, to accommodate more wind energy throughout the scheduling horizon. In fact, all aggregated conventional power output curves adhere better to the net-load

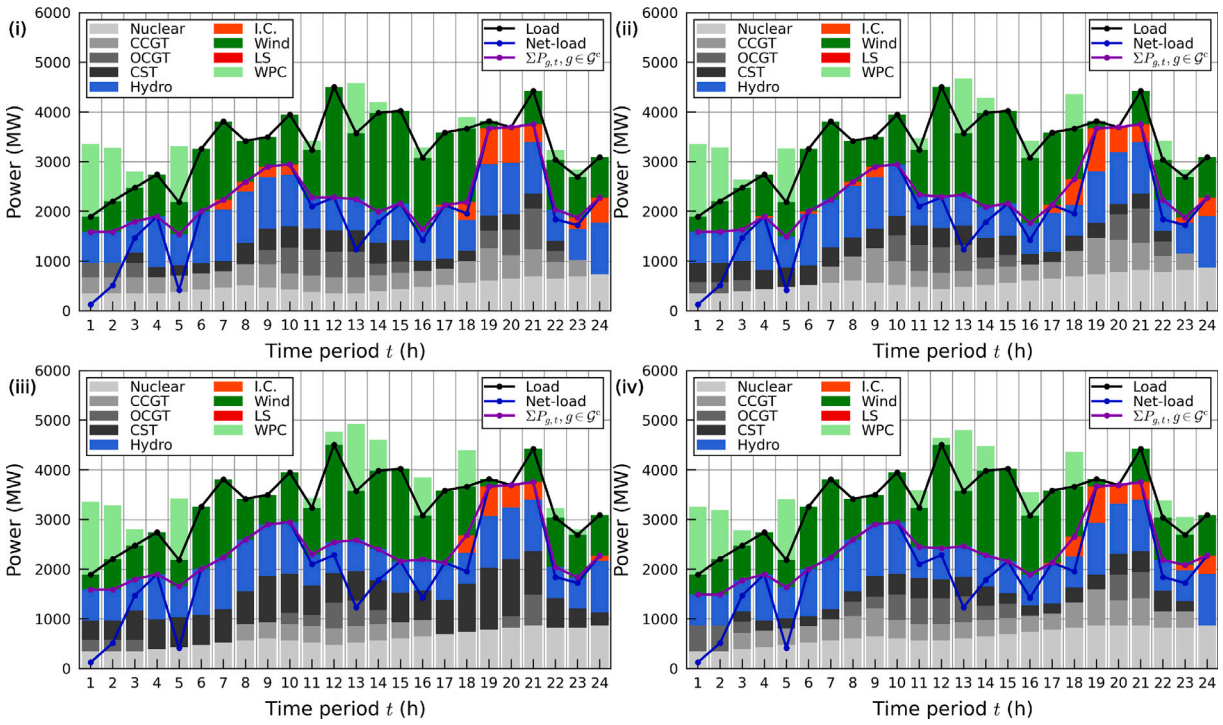

Fig. 10. Aggregated power dispatching by generation technology. Representative scenario $\xi = 7$. Best-compromise solutions.

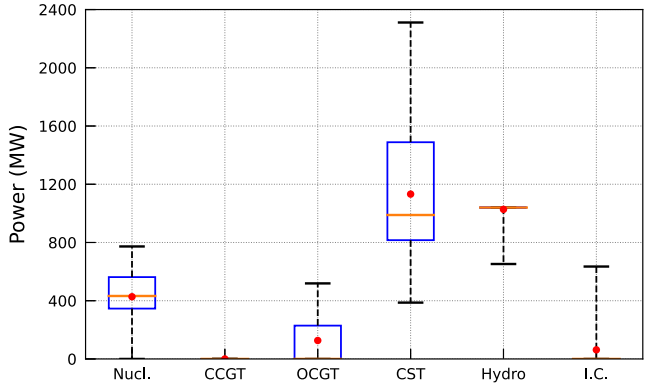

Fig. 11. Hourly power production by conventional generation technology within the scheduling horizon. Optimal min. $\mathbf{E}(C^T_\xi)$ solution.

curve, the level of adherence depending on the relative importance of wind power curtailment performance and how this is achieved depending on the relative importance of operating cost and CO_2 performance. For instance best-compromise solutions (i) and (ii), offer the lower wind energy curtailment rates for scenario $\xi = 7$, 20.15% and 22.84%, respectively, in accordance with the relative importance of wind power curtailment, but solution (i) is 3.53% more expensive than solution (ii), and presents 0.32% less of CO_2 emissions, coherently with the relative importance of those objectives in each case. The slight differences between these solutions lie in the extent of use of coal-based CST and gas-based CCGT technologies. Indeed, best-compromise solution (i) has the concurrent requirements of reducing CO_2 emissions and wind power curtailment, causing a more intensive use of gas-based CCGT with respect to coal-based CST, being the former technology more flexible than the latter, but more expensive due to its increased O&M and fuel costs. Similar implications are found for best-compromised solutions (iii) and (iv), that privilege more acutely the operating cost and CO_2 emissions performance, respectively. Solution (iii) shows a more predominant use of coal-based CST replacing gas-based CCGT and even gas-based OCGT, whereas solution (iv) shows the opposite in addition to a more reduced use of the I.C., which is also a CO_2 emitting source.

Analogously to the minimum cost solution case, the above insights on the best-compromise solutions for representative scenario $\xi = 7$ can be extrapolated to all the representative scenarios considered. This is supported by the weighted box plots in Fig. 12, presenting the hourly power production of each conventional generation technology within the scheduling horizon for the best-compromise solutions.

It is worth remarking that by means of the proposed CP framework, we provide a useful spectrum of information to the DM by designing best-compromise on/off schedules according to his/her preferences. As discussed before, the final decision will depend on the goals of the DM and the operating cost performance sacrifice that he/she is willing to make in order to improve CO_2 emissions and wind power curtailment performance. It is also important to recall that these potential improvements are achieved solely by modifying the operational strategy. In this view, it results of interest to extend and apply the proposed CP framework to analyze the potential contributions of investment decisions, including energy storage technologies, on the design and operation of sustainable power systems. Moreover, the proposed CP framework can be also used to study the impact of carbon taxation policies on CO_2 emissions, i.e., how the inclusion of a carbon tax in the cost-based objective function affects the trade-off between operating cost, CO_2 emissions and wind power curtailment performance, and determine the adequate level for it.

In relation to the computational efficiency of the proposed CP framework, Fig. 13 presents the total wall-clock time in seconds (dashed line, right y-axis) and the % of the total wall-clock time (bars, left y-axis) by type of subproblem, for runs with $|\Omega| = \{3, 7, 15, 25\}$ representative operational scenarios. It can be observed the expected exponential increments of the total wall-clock time with respect to the number of scenarios. It must noticed that, for the presented case study with $|\Omega| = 25$ representative operational scenarios, the implementation of the proposed CP framework subscribes 3.88 hours (13966 s) of computation. This time is reasonable considering the operating nature

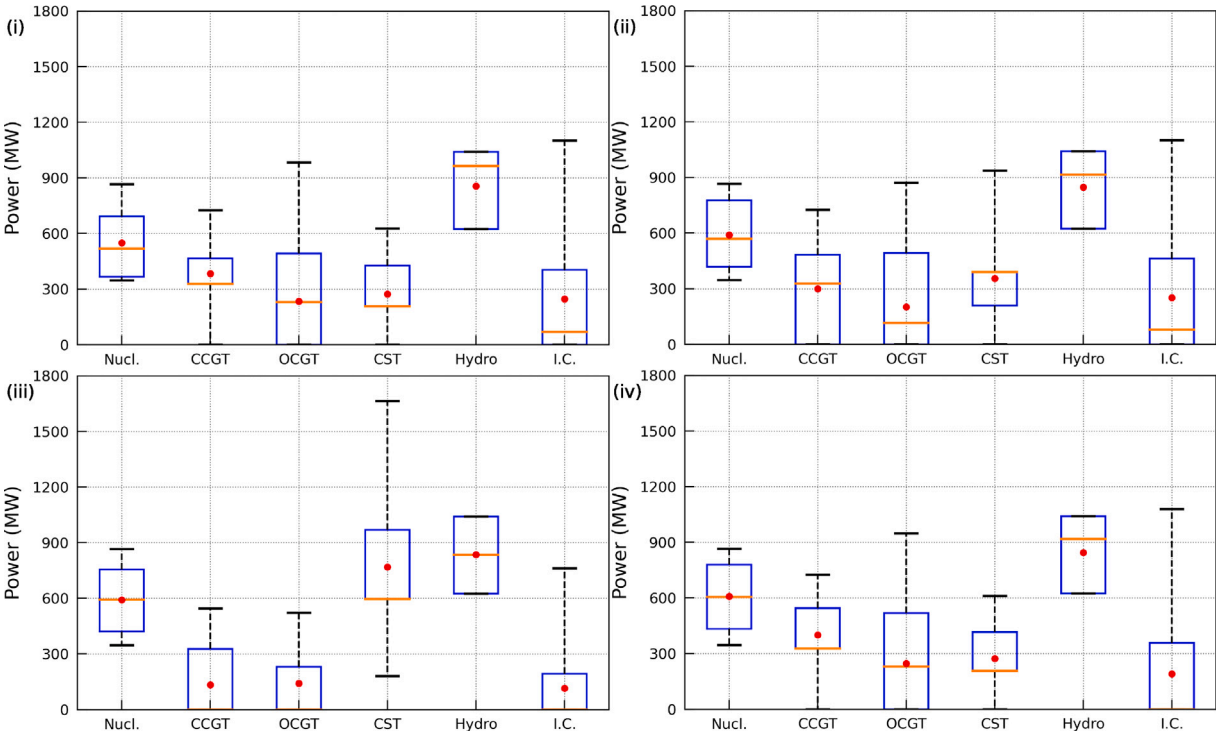

Fig. 12. Hourly power production by conventional generation technology within the scheduling horizon. Best-compromise solutions.

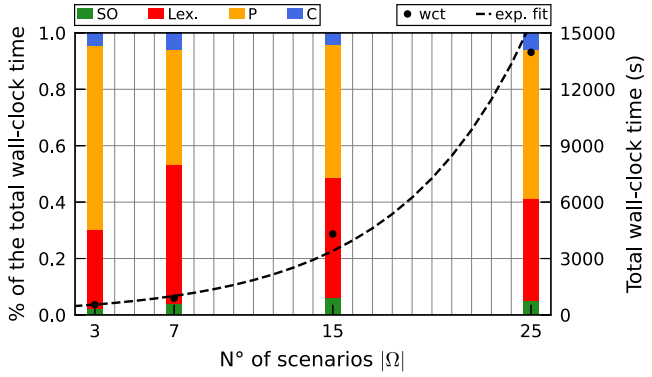

Fig. 13. Total wall-clock time (right y-axis) and % of the total wall-clock time (left y-axis) vs n° of scenarios.

of the problem and the relative small size of the IEEE-39 bus test system regarding the number of conventional generation units. We must recall and remark, however, that the proposed framework relies on the deterministic equivalent or extensive formulation of the two-stage stochastic UC problem, which is restrictive in terms of computational efficiency. Although the framework can be applied to larger systems in reasonable computational times, e.g., by significantly reducing the number of representatives scenarios considered [22] and/or reducing the number of 2-Pareto solution for estimating the Nadir point, this is done to the detriment of the representativeness of the optimal solutions.

On the basis of the above, the next stage of development should account for replacing the use and resolution of the deterministic equivalent of the stochastic UC problem by more sophisticated and efficient exact methods of solution that profit from its structure. In fact, the implementation of the framework considers the exact resolution of 34 MILP (sub)problems in total (see Fig. 13): 3 single-objective problems for each objective function (SO, green bar), $3 \times 2 = 6$ lexicographic problems to determine the 2-Pareto optimal extreme solutions (Lex., red bar), $3 \times 7 = 21$ ϵ-constrained problems to determine the intermediate 2-Pareto optimal solutions (P, orange bar), and 4 problems to determine the best-compromised solutions (C, blue bar). As it can be observed in Fig. 13, most of the computational effort is invested in the resolution of lexicographic and ϵ-constrained problems which present hard expected values constraints. This computational challenge can be effectively addressed by means of Bender's type decomposition [61] and/or decomposition based on Lagrangian relaxation [62] conjointly with parallel computing.

5. Conclusions

In this paper, we have presented a compromise programming optimization framework for a multi-objective two-stage stochastic unit commitment model for power systems with high shares of wind energy. The proposed framework aims at finding Pareto optimal on/off schedules to the two-stage stochastic unit commitment problem that trade-off, based on the decision maker's preferences, three conflicting objectives, namely, expected operating cost, expected CO_2 emissions and expected wind power curtailment performance. This is done under the realistic assumption that for the given multi-objective two-stage stochastic unit commitment model, the decision maker seeks Pareto optimal schedules as close as possible to the ideal point, i.e., to the theoretical point where the three objectives are concurrently minimized, and as far as possible to the anti-ideal or Nadir point, i.e., to the point where the three objectives are simultaneously maximized. To achieve this, we have presented a comprehensible and practical procedure to compute the ideal and Nadir points, and the trade-off ranges of each objective function, associated to the two-stage stochastic unit commitment problem, based on an augmented ϵ-constrained method that integrates a normalized Euclidean distance-based bisection routine. In addition, we have proposed a weighted ℓ_1 norm-based linearized compromise program that allows to design best-compromise on/off schedules that minimize/maximize their distances to the ideal/Nadir point in accordance to the decision maker's preferences, which are represented by weights standing for the relative importance of the three objectives considered.

All optimization problems involved in the proposed framework correspond to mixed-integer linear programming instances of the two-stage stochastic unit commitment model and are solved through traditional exact methods. The uncertain parameters taken into account are the aggregated demand of the system and the wind speed profiles for which diverse scenarios are sampled. To reduce the computational burden of the framework, we implement a scenario-reduction technique based on the unsupervised k-means clustering method, to determine a set of representative operational scenarios and to estimate their corresponding probability of occurrence.

A case study, based on a modification of the New England IEEE-39 bus test system, has been analyzed. The obtained results show the effectiveness of the proposed framework in designing best-compromise Pareto optimal schedules for diverse settings of the DM's preferences. A comparative analysis between the designed best-compromise schedules and the traditional minimum expected operating cost schedule shows that considerable simultaneous reductions in expected CO_2 emissions and expected wind power curtailment performance can be attained by conservatively sacrificing expected operating cost performance. In addition, the contribution of each type of generation technology on this trade-off has been analyzed, providing meaningful insights on the role that low-carbon flexible generation technologies play in the development of more sustainable operation strategies. In this view, through the proposed framework, a comprehensible spectrum of information can be supplied to the DM in support to his/her decision task in accordance to his/her preferences and goals.

Future work includes the design and implementation of decomposition methods to reduce the computational burden of the framework. This would allow to extend it for studying the potential contribution of investment decisions on the trade-off between operating cost, CO_2 emissions and wind power curtailment performance in transmission network-constrained settings. Furthermore, the proposed compromise programming optimization framework will be used to study the impact of carbon taxation policies on the trade-off of the mentioned three objectives and how to determine a proper level for the carbon tax.

CRediT authorship contribution statement

R. Mena: Conceptualization, Methodology, Software, Validation, Formal analysis, Investigation, Resources, Data curation, Writing – original draft, Visualization, Supervision, Project administration, Funding acquisition, Writing – review & editing. **M. Godoy:** Conceptualization, Methodology, Software, Validation, Formal analysis, Data curation, Writing – original draft, Visualization. **C. Catalán:** Conceptualization, Methodology, Software, Validation. **P. Viveros:** Formal analysis, Resources, Visualization, Writing – review & editing. **E. Zio:** Formal analysis, Writing – review & editing.

Declaration of competing interest

The authors declare that they have no known competing financial interests or personal relationships that could have appeared to influence the work reported in this paper.

Data availability

Data will be made available on request

Acknowledgments

We would like to thank the support of the Agencia Nacional de Investigación y Desarrollo (ANID) through the Fondo Nacional de Desarrollo Científico Y Tecnológico (FONDECYT), project 11190269.

Appendix

Lexicographic optimality

Let $\mathbf{z}^1$ and $\mathbf{z}^2$ two vectors in $\mathbb{R}^K$. Then, $\mathbf{z}^1$ is lexicographically less than $\mathbf{z}^2$, denoted $\mathbf{z}^1 <_\ell \mathbf{z}^2$ if $\exists k \in \{1,\dots,K\}$ such that $\mathbf{z}^1_j = \mathbf{z}^2_j, \forall j \in \{1,\dots,k-1\}$ and $\mathbf{z}^1_k = \mathbf{z}^2_k$. $\mathbf{z}^1$ is lexicographically less than or equal to $\mathbf{z}^2$, denoted $\mathbf{z}^1 \leq_\ell \mathbf{z}^2$ if $\mathbf{z}^1 <_\ell \mathbf{z}^2$ or $\mathbf{z}^1 = \mathbf{z}^2$ [63].

Let $\pi = (\pi(1),\dots,\pi(K))$ be a permutation of the set $\{1,\dots,K\}$, then, a feasible solution $\mathbf{x}^{*\pi}$ of the problem (MOOP) is called lexicographically optimal with respect to the permutation π of objective functions order if $f_\pi(\mathbf{x}^{*\pi}) \leq_\ell f_\pi(\mathbf{x}), \forall x \in \mathcal{D}$, where $f_\pi(\mathbf{x}) = (f_{\pi(1)}(\mathbf{x}),\dots,f_{\pi(K)}(\mathbf{x}))$. Moreover, any feasible solution of the problem (MOOP) $\mathbf{x}^*$ is called global lexicographically optimal if there exist a permutation π such that $\mathbf{x}^*$ is lexicographically optimal with respect to π [39].

Linearized CSP

The linearization (l-CSP) of the (CSP) for the ℓ_1 norm can be formulated as:

$$\begin{aligned}
\min_{\mathbf{x}} \quad & \left(\sum_{k=1}^{K} w_k^p \left|\frac{f_k(\mathbf{x}) - f_k^{\mathrm{I}}}{f_k^{\mathrm{N}} - f_k^{\mathrm{I}}}\right|^p\right)^{1/p} - \left(\sum_{k=1}^{K} w_k^p \left|\frac{f_k^{\mathrm{N}} - f_k(\mathbf{x})}{f_k^{\mathrm{N}} - f_k^{\mathrm{I}}}\right|^p\right)^{1/p} \\
\text{s.t.} \quad & f_k(\mathbf{x}) \leq f_k^{\mathrm{N}}, \quad \forall k \in \{1,\dots,K\} \\
& \mathbf{x} \in \mathcal{D}
\end{aligned} \tag{CSP}$$

$$\begin{aligned}
\min_{\mathbf{x}} \quad & \sum_{k=1}^{K} w_k \frac{(d_k^{+\mathrm{I}} + d_k^{-\mathrm{I}}) - (d_k^{+\mathrm{N}} + d_k^{-\mathrm{N}})}{f_k^{\mathrm{N}} - f_k^{\mathrm{I}}} \\
\text{s.t.} \quad & f_k(\mathbf{x}) \leq f_k^{\mathrm{N}}, \quad \forall k \in \{1,\dots,K\} \\
& d_k^{+\mathrm{I}} - d_k^{-\mathrm{I}} = f_k(\mathbf{x}) - f_k^{\mathrm{I}}, \quad \forall k \in \{1,\dots,K\} \\
& d_k^{+\mathrm{N}} - d_k^{-\mathrm{N}} = f_k^{\mathrm{N}} - f_k(\mathbf{x}), \quad \forall k \in \{1,\dots,K\} \\
& d_k^{+\mathrm{I}}, d_k^{-\mathrm{I}}, d_k^{+\mathrm{N}}, d_k^{-\mathrm{N}} \geq 0, \quad \forall k \in \{1,\dots,K\} \\
& \mathbf{x} \in \mathcal{D}
\end{aligned} \tag{l-CSP}$$

References

[1] IEA. Renewables 2021. Int Energy Agency (IEA) Publ Int 2021;167, URL www.iea.org/t&c/%0Ahttps://webstore.iea.org/download/direct/4329.

[2] Agency IE. Global Energy Review : CO2 Emissions in 2021 Global emissions rebound sharply to highest ever level international energy. 2021.

[3] Zhou B, Fang J, Ai X, Yao W, Wen J. Flexibility-enhanced continuous-time scheduling of power system under wind uncertainties. IEEE Trans Sustain Energy 2021;12(4):2306–20. http://dx.doi.org/10.1109/TSTE.2021.3089696.

[4] Morales-España G, Nycander E, Sijm J. Reducing CO2 emissions by curtailing renewables: Examples from optimal power system operation. Energy Econ 2021;99:105277. http://dx.doi.org/10.1016/j.eneco.2021.105277, URL https://www.sciencedirect.com/science/article/pii/S0140988321001821.

[5] Abujarad SY, Mustafa MW, Jamian JJ. Recent approaches of unit commitment in the presence of intermittent renewable energy resources: A review. Renew Sustain Energy Rev 2017;70:215–23. http://dx.doi.org/10.1016/j.rser.2016.11.246, URL https://www.sciencedirect.com/science/article/pii/S1364032116310140.

[6] Postolov B, Iliev A. New metaheuristic methodology for solving security constrained hydrothermal unit commitment based on adaptive genetic algorithm. Int J Electr Power Energy Syst 2022;134:107163. http://dx.doi.org/10.1016/j.ijepes.2021.107163, URL https://www.sciencedirect.com/science/article/pii/S0142061521004026.

[7] Gentile C, Morales-España G, Ramos A. A tight MIP formulation of the unit commitment problem with start-up and shut-down constraints. EURO J Comput Optim 2017;5(1):177–201. http://dx.doi.org/10.1007/s13675-016-0066-y, URL https://www.sciencedirect.com/science/article/pii/S2192440621000782.

[8] Akhlaghi M, Moravej Z, Bagheri A. Maximizing wind energy utilization in smart power systems using a flexible network-constrained unit commitment through dynamic lines and transformers rating. Energy 2022;261:124918. http://dx.doi.org/10.1016/j.energy.2022.124918, URL https://www.sciencedirect.com/science/article/pii/S0360544222018199.

[9] Yang B, Cao X, Cai Z, Yang T, Chen D, Gao X, et al. Unit commitment comprehensive optimal model considering the cost of wind power curtailment and deep peak regulation of thermal unit. IEEE Access 2020;8:71318–25. http://dx.doi.org/10.1109/ACCESS.2020.2983183.

[10] Jain A, Yamujala S, Das P, Gaur AS, Bhakar R, Mathur J, et al. Unit commitment framework to assess flexibility resource capability for high RE penetration. In: 2020 IEEE PES innovative smart grid technologies Europe (ISGT-Europe). 2020, p. 779–83. http://dx.doi.org/10.1109/ISGT-Europe47291.2020.9248969.

[11] Dhaliwal JS, Dhillon JS. Memetic binary differential evolution to solve wind–thermal profit based unit commitment problem. Appl Soft Comput 2022;125:109105. http://dx.doi.org/10.1016/j.asoc.2022.109105, URL https://www.sciencedirect.com/science/article/pii/S1568494622003842.

[12] Wang S, Xu X, Kong X, Yan Z. Extended priority list and discrete heuristic search for multi-objective unit commitment. Int Trans Electr Energy Syst 2018;28(2):e2486. http://dx.doi.org/10.1002/etep.2486, e2486 ITEES-17-0257.R2. URL arXiv:https://onlinelibrary.wiley.com/doi/pdf/10.1002/etep.2486, https://onlinelibrary.wiley.com/doi/abs/10.1002/etep.2486.

[13] Li Y-F, Pedroni N, Zio E. A memetic evolutionary multi-objective optimization method for environmental power unit commitment. IEEE Trans Power Syst 2013;28(3):2660–9. http://dx.doi.org/10.1109/TPWRS.2013.2241795.

[14] Yang D, Zhou X, Yang Z, Guo Y, Niu Q. Low carbon multi-objective unit commitment integrating renewable generations. IEEE Access 2020;8:207768–78. http://dx.doi.org/10.1109/ACCESS.2020.3022245.

[15] Narimani H, Azizivahed A, Naderi E, Fathi M, Narimani MR. A practical approach for reliability-oriented multi-objective unit commitment problem. Appl Soft Comput 2019;85:105786. http://dx.doi.org/10.1016/j.asoc.2019.105786, URL https://www.sciencedirect.com/science/article/pii/S1568494619305678.

[16] Chandrasekaran K, Simon SP. Optimal deviation based firefly algorithm tuned fuzzy design for multi-objective UCP. IEEE Trans Power Syst 2013;28(1):460–71. http://dx.doi.org/10.1109/TPWRS.2012.2201963.

[17] Zhu Y, Liu X, Deng R, Zhai Y. Memetic algorithm for solving monthly unit commitment problem considering uncertain wind power. J Control Autom Electr Syst 2020;31(2):511–20. http://dx.doi.org/10.1007/s40313-019-00541-3, URL https://doi.org/10.1007/s40313-019-00541-3.

[18] Li J, Zhou S, Xu Y, Zhu M, Ye L. A multi-band uncertainty set robust method for unit commitment with wind power generation. Int J Electr Power Energy Syst 2021;131:107125. http://dx.doi.org/10.1016/j.ijepes.2021.107125, URL https://www.sciencedirect.com/science/article/pii/S0142061521003641.

[19] Mingtao L, Xionghua S, Yong B, Yongtian J, Wei G, Jun X. A emission-constrained unit commitment model considering randomness of wind power and electric vehicle. In: 2021 IEEE sustainable power and energy conference. ISPEC, 2021, p. 490–5. http://dx.doi.org/10.1109/iSPEC53008.2021.9735884.

[20] Huang Y, Xu Q, Xia Y, Yue D, Dou C. Wind–thermal power generation scheduling with predictive transmission security margin. Int J Electr Power Energy Syst 2022;141:108197. http://dx.doi.org/10.1016/j.ijepes.2022.108197, URL https://www.sciencedirect.com/science/article/pii/S0142061522002307.

[21] Nikoobakht A, Aghaei J, Shafie-Khah M, Catalão JPS. Minimizing wind power curtailment using a continuous-time risk-based model of generating units and bulk energy storage. IEEE Trans Smart Grid 2020;11(6):4833–46. http://dx.doi.org/10.1109/TSG.2020.3004488.

[22] Zhang M, Zhou M, Li G, Sun Y. Quantifying accommodated domain of wind power for flexible look-ahead unit commitment. Electr Power Syst Res 2020;187:106471. http://dx.doi.org/10.1016/j.epsr.2020.106471, URL https://www.sciencedirect.com/science/article/pii/S0378779620302753.

[23] Naghdalian S, Amraee T, Kamali S, Capitanescu F. Stochastic network-constrained unit commitment to determine flexible ramp reserve for handling wind power and demand uncertainties. IEEE Trans Ind Inf 2020;16(7):4580–91. http://dx.doi.org/10.1109/TII.2019.2944234.

[24] Zhang H, Hu X, Cheng H, Zhang S, Hong S, Gu Q. Coordinated scheduling of generators and tie lines in multi-area power systems under wind energy uncertainty. Energy 2021;222:119929. http://dx.doi.org/10.1016/j.energy.2021.119929, URL https://www.sciencedirect.com/science/article/pii/S036054422100178X.

[25] Fang Y, Zhao S, Chen Z. Multi-objective unit commitment of jointly concentrating solar power plant and wind farm for providing peak-shaving considering operational risk. Int J Electr Power Energy Syst 2022;137:107754. http://dx.doi.org/10.1016/j.ijepes.2021.107754, URL https://www.sciencedirect.com/science/article/pii/S0142061521009765.

[26] Wang B, Wang S, Zhou X-z, Watada J. Two-stage multi-objective unit commitment optimization under hybrid uncertainties. IEEE Trans Power Syst 2016;31(3):2266–77. http://dx.doi.org/10.1109/TPWRS.2015.2463725.

[27] Li Y, Li H, Wang B, Zhou M, Jin M. Multi-objective unit commitment optimization with ultra-low emissions under stochastic and fuzzy uncertainties. Int J Mach Learn Cybern 2021;12(1):1–15. http://dx.doi.org/10.1007/s13042-020-01103-9, URL https://doi.org/10.1007/s13042-020-01103-9.

[28] Wang B, Wang S, Zhou X, Watada J. Multi-objective unit commitment with wind penetration and emission concerns under stochastic and fuzzy uncertainties. Energy 2016;111:18–31. http://dx.doi.org/10.1016/j.energy.2016.05.029, URL https://www.sciencedirect.com/science/article/pii/S0360544216305813.

[29] Xie M, Yan Y, Ke S, Liu M. Vector ordinal optimization theory based large-scale multi-objective unit commitment considering stochastic wind power. IEEJ Trans Electr Electron Eng 2018;13(3):463–71. http://dx.doi.org/10.1002/tee.22589, URL arXiv:https://onlinelibrary.wiley.com/doi/pdf/10.1002/tee.22589, https://onlinelibrary.wiley.com/doi/abs/10.1002/tee.22589.

[30] Braga Flôr VB, Do Coutto Filho MB, Stachinni de Souza JC, Satoru Ochi L. Strategic observation of power grids for reliable monitoring. Int J Electr Power Energy Syst 2022;138:107959. http://dx.doi.org/10.1016/j.ijepes.2022.107959, URL https://www.sciencedirect.com/science/article/pii/S0142061522000060.

[31] Jiménez-Cordero A, Morales JM, Pineda S. Warm-starting constraint generation for mixed-integer optimization: A machine learning approach. Knowl-Based Syst 2022;253:109570. http://dx.doi.org/10.1016/j.knosys.2022.109570, URL https://www.sciencedirect.com/science/article/pii/S0950705122007894.

[32] Furukakoi M, Adewuyi OB, Matayoshi H, Howlader AM, Senjyu T. Multi objective unit commitment with voltage stability and PV uncertainty. Appl Energy 2018;228:618–23. http://dx.doi.org/10.1016/j.apenergy.2018.06.074, URL https://www.sciencedirect.com/science/article/pii/S0306261918309450.

[33] Mavrotas G. Effective implementation of the ϵ-constraint method in multi-objective mathematical programming problems. Appl Math Comput 2009;213(2):455–65. http://dx.doi.org/10.1016/j.amc.2009.03.037, URL https://www.sciencedirect.com/science/article/pii/S0096300309002574.

[34] Ruiz AB, Saborido R, Luque M. A preference-based evolutionary algorithm for multiobjective optimization: The weighting achievement scalarizing function genetic algorithm. J Global Optim 2015;62(1):101–29. http://dx.doi.org/10.1007/s10898-014-0214-y, URL http://link.springer.com/10.1007/s10898-014-0214-y.

[35] Hajebrahimi A, Abdollahi A, Rashidinejad M. Probabilistic multiobjective transmission expansion planning incorporating demand response resources and large-scale distant wind farms. IEEE Syst J 2017;11(2):1170–81. http://dx.doi.org/10.1109/JSYST.2015.2464151.

[36] Mena R, Zio E, Viveros P. Matérn process-based simulation of wind speed time series. Energy Convers Manage 2022;266:115596. http://dx.doi.org/10.1016/j.enconman.2022.115596, URL https://www.sciencedirect.com/science/article/pii/S0196890422003922.

[37] Morales-España G, Latorre JM, Ramos A. Tight and compact MILP formulation for the thermal unit commitment problem. IEEE Trans Power Syst 2013;28(4):4897–908. http://dx.doi.org/10.1109/TPWRS.2013.2251373.

[38] Branke J, Deb K, Miettinen K, Slowinski R. Multiobjective optimization: Interactive and evolutionary Approaches. LNCS sublibrary: Theoretical computer science and general issues, Springer; 2008, URL http://books.google.fr/books?id=N-1hWMNUa2EC.

[39] Ehrgott M, Tenfelde-Podehl D. Computation of ideal and nadir values and implications for their use in MCDM methods. European J Oper Res 2003;151(1):119–39. http://dx.doi.org/10.1016/S0377-2217(02)00595-7, URL https://www.sciencedirect.com/science/article/pii/S0377221702005957.

[40] Romero C, Rehman T, editors. Chapter five compromise programming. In: Multiple criteria analysis for agricultural decisions, developments in agricultural economics, Vol. 11. Elsevier; 2003, p. 63–78. http://dx.doi.org/10.1016/S0926-5589(03)80007-9, URL https://www.sciencedirect.com/science/article/pii/S0926558903800079.

[41] Carpinelli G, Caramia P, Mottola F, Proto D. Exponential weighted method and a compromise programming method for multi-objective operation of plug-in vehicle aggregators in microgrids. Int J Electr Power Energy Syst 2014;56:374–84. http://dx.doi.org/10.1016/j.ijepes.2013.11.036, URL https://www.sciencedirect.com/science/article/pii/S0142061513004948.

[42] Chancelier J-P, de Lara M. Orthant-strictly monotonic norms, generalized top-k and k-support norms and the L0 pseudonorm. 2020, http://dx.doi.org/10.48550/ARXIV.2001.10441, URL https://arxiv.org/abs/2001.10441.

[43] Zhang W, Reimann M. A simple augmented ϵ-constraint method for multi-objective mathematical integer programming problems. European J Oper Res 2014;234(1):15–24. http://dx.doi.org/10.1016/j.ejor.2013.09.001, URL https://www.sciencedirect.com/science/article/pii/S0377221713007376.

[44] Zardari NH, Ahmed K, Shirazi S, Yusop Z. Weighting methods and their effects on multi-criteria decision making model outcomes in water resources management. Springer; 2015, http://dx.doi.org/10.1007/978-3-319-12586-2.

[45] Zhang H, Lu M, Ke X, Yu S, Zhao J, Wu Y, et al. Evaluation model of black-start schemes based on optimal combination weights and improved VIKOR method. Int J Electr Power Energy Syst 2021;129:106762. http://dx.doi.org/10.1016/j.ijepes.2021.106762, URL https://www.sciencedirect.com/science/article/pii/S0142061521000028.

[46] Namilakonda S, Guduri Y. Chaotic darwinian particle swarm optimization for real-time hierarchical congestion management of power system integrated with renewable energy sources. Int J Electr Power Energy Syst 2021;128:106632. http://dx.doi.org/10.1016/j.ijepes.2020.106632, URL https://www.sciencedirect.com/science/article/pii/S0142061520341776.

[47] Hart WE, Watson J-P, Woodruff DL. Pyomo: Modeling and solving mathematical programs in Python. Math Program Comput 2011;3(3):219–60.

[48] Gurobi Optimization L. Gurobi optimizer reference manual. 2022, URL https://www.gurobi.com.

[49] MatPower. CASE39 power flow data for 39 bus new england system. 2014, [Last access november 2019] 2014.

[50] USEnergy Information Adminstration (EIA). Electric power annual 2018. Tech. Rep., (October):2019, p. 1–239.

[51] Yehescale G, Reddy MD. A new strategy for solving unit commitment problem by PSO algorithm. In: 2018 IEEE international conference on current trends in advanced computing. ICCTAC, IEEE; 2018, p. 1–6.

[52] Van den Bergh K, Delarue E. Cycling of conventional power plants: Technical limits and actual costs. Energy Convers Manage 2015;97:70–7. http://dx.doi.org/10.1016/j.enconman.2015.03.026, URL https://www.sciencedirect.com/science/article/pii/S0196890415002368.

[53] Vestas wind turbines. V90e2.0 technical specifications (Online).URL http://www.vestas.com.

[54] Bonneville Power Administration (BPA). Meteorological Data from BPA Sites (Online).URL https://transmission.bpa.gov/Business/Operations/Wind/.

[55] Gualtieri G, Secci S. Methods to extrapolate wind resource to the turbine hub height based on power law: A 1-h wind speed vs. Weibull distribution extrapolation comparison. Renew Energy 2012;43:183–200. http://dx.doi.org/10.1016/j.renene.2011.12.022, URL https://www.sciencedirect.com/science/article/pii/S0960148112000109.

[56] IRENA. Renewable energy technologies: Cost analysis series, volume 1: Power sector. Tech. Rep., 2012.

[57] Dvorkin Y, Wang Y, Pandzic H, Kirschen D. Comparison of scenario reduction techniques for the stochastic unit commitment. In: 2014 IEEE pes general meeting | conference & exposition. 2014, p. 1–5. http://dx.doi.org/10.1109/PESGM.2014.6939042.

[58] Baringo L, Conejo AJ. Risk-constrained multi-stage wind power investment. In: 2014 IEEE pes general meeting | conference & exposition. 2014, p. 1. http://dx.doi.org/10.1109/PESGM.2014.6938904.

[59] Yasuda Y, Bird L, Carlini EM, Eriksen PB, Estanqueiro A, Flynn D, et al. C-e (curtailment – energy share) map: An objective and quantitative measure to evaluate wind and solar curtailment. Renew Sustain Energy Rev 2022;160:112212. http://dx.doi.org/10.1016/j.rser.2022.112212, URL https://www.sciencedirect.com/science/article/pii/S1364032122001356.

[60] Niu T, Guo Q, Sun H, Wang B, Zhang B. Voltage security regions considering wind power curtailment to prevent cascading trip faults in wind power integration areas. IET Renew Power Gener 2017;11(1):54–62. http://dx.doi.org/10.1049/iet-rpg.2016.0151, URL arXiv:https://ietresearch.onlinelibrary.wiley.com/doi/pdf/10.1049/iet-rpg.2016.0151 https://ietresearch.onlinelibrary.wiley.com/doi/abs/10.1049/iet-rpg.2016.0151.

[61] Colonetti B, Finardi E, Larroyd P, Beltrán F. A novel cooperative multi-search benders decomposition for solving the hydrothermal unit-commitment problem. Int J Electr Power Energy Syst 2022;134:107390. http://dx.doi.org/10.1016/j.ijepes.2021.107390, URL https://www.sciencedirect.com/science/article/pii/S0142061521006293.

[62] Reolon Scuzziato M, Cristian Finardi E, Frangioni A. Solving stochastic hydrothermal unit commitment with a new primal recovery technique based on Lagrangian solutions. Int J Electr Power Energy Syst 2021;127:106661. http://dx.doi.org/10.1016/j.ijepes.2020.106661, URL https://www.sciencedirect.com/science/article/pii/S014206152034206X.

[63] Mäkelä MM, Nikulin Y. Properties of efficient solution sets under addition of objectives. Oper Res Lett 2008;36(6):718–21. http://dx.doi.org/10.1016/j.orl.2008.07.006, URL https://www.sciencedirect.com/science/article/pii/S0167637708000928.